The Plant Cell, Vol. 13, 853–871, April 2001, www.plantcell.org © 2001 American Society of Plant Physiologists

The *TRANSPARENT TESTA12* Gene of Arabidopsis Encodes a Multidrug Secondary Transporter-like Protein Required for Flavonoid Sequestration in Vacuoles of the Seed Coat Endothelium

Isabelle Debeaujon,[1] Anton J. M. Peeters,[2] Karen M. Léon-Kloosterziel,[3] and Maarten Koornneef[4]

Laboratory of Genetics, Graduate School of Experimental Plant Sciences, Wageningen University, Dreijenlaan 2, 6703 HA Wageningen, The Netherlands

Phenolic compounds that are present in the testa interfere with the physiology of seed dormancy and germination. We isolated a recessive Arabidopsis mutant with pale brown seeds, *transparent testa12* (*tt12*), from a reduced seed dormancy screen. Microscopic analysis of *tt12* developing and mature testas revealed a strong reduction of proanthocyanidin deposition in vacuoles of endothelial cells. Double mutants with *tt12* and other testa pigmentation mutants were constructed, and their phenotypes confirmed that *tt12* was affected at the level of the flavonoid biosynthetic pathway. The *TT12* gene was cloned and found to encode a protein with similarity to prokaryotic and eukaryotic secondary transporters with 12 transmembrane segments, belonging to the MATE (multidrug and toxic compound extrusion) family. *TT12* is expressed specifically in ovules and developing seeds. In situ hybridization localized its transcript in the endothelium layer, as expected from the effect of the *tt12* mutation on testa flavonoid pigmentation. The phenotype of the mutant and the nature of the gene suggest that TT12 may control the vacuolar sequestration of flavonoids in the seed coat endothelium.

INTRODUCTION

Flavonoids represent a highly diverse group of plant aromatic secondary metabolites. The major forms, which are anthocyanins (red to purple pigments), flavonols (colorless to pale yellow pigments), and proanthocyanidins (PAs), also known as condensed tannins (colorless pigments that brown with oxidation), are present in proportions and amounts that vary according to the plant species, the organ, the stage of development, and environmental growth conditions. Arabidopsis contains flavonoid pigments in vegetative tissues and in seeds (Shirley et al., 1995). In the mature testa, flavonoids were detected in both the endothelium and the three crushed parenchymal layers just above the endothelium (Debeaujon et al., 2000). PAs have been shown to accumulate exclusively in the endothelium layer (Devic et al., 1999). Wild-type seed color depends on the stage of development: as long as the testa is transparent, until ~10 days after pollination, the seed has the color of the underlying endosperm and embryo. At maturity, the testa becomes opaque after the oxidation of flavonoid pigments, which gives the seed its characteristic brown color. Therefore, the color of mutants with seed flavonoid defects ranges from pale yellow (complete lack of visible pigments in the testa) to pale brown, depending on the accumulated intermediate flavonoids (Debeaujon et al., 2000).

In Arabidopsis, mutants at 21 loci have been isolated on the basis of altered testa pigmentation (Figure 1). The genes disrupted in the *transparent testa* (*tt*) mutants *tt3*, *tt4*, *tt5*, *tt6*, and *tt7* (Shirley et al., 1995) and the *banyuls* (*ban*) mutant (Albert et al., 1997) code for the enzymes dihydroflavonol-4-reductase (Shirley et al., 1992), chalcone synthase (Feinbaum and Ausubel, 1988), chalcone isomerase (Shirley et al., 1992), flavonol 3-hydroxylase (Pelletier and Shirley, 1996; Wisman et al., 1998), flavonol 3′-hydroxylase (Koornneef et al., 1982; Schoenbohm et al., 2000), and leucoanthocyanidin reductase (Devic et al., 1999), respectively. In addition, several regulatory mutants and their corresponding genes have been identified. These are the *tt8*, *transparent testa glabra1* (*ttg1*) (Shirley et al., 1995) and *ttg2* (C.J. Johnson

[1] Current address: Laboratoire de Biologie des Semences, Institut National de la Recherche Agronomique, Route de Saint-Cyr, 78026 Versailles cedex, France.
[2] Current address: Department of Plant Ecophysiology, Utrecht University, Sorbonnelaan 16, 3584 CA, Utrecht, The Netherlands.
[3] Current address: Department of Plant Pathology, Utrecht University, Sorbonnelaan 16, 3584 CA, Utrecht, The Netherlands.
[4] To whom correspondence should be addressed. E-mail maarten.koornneef@genetics.dpw.wau.nl; fax 31-317-483146.

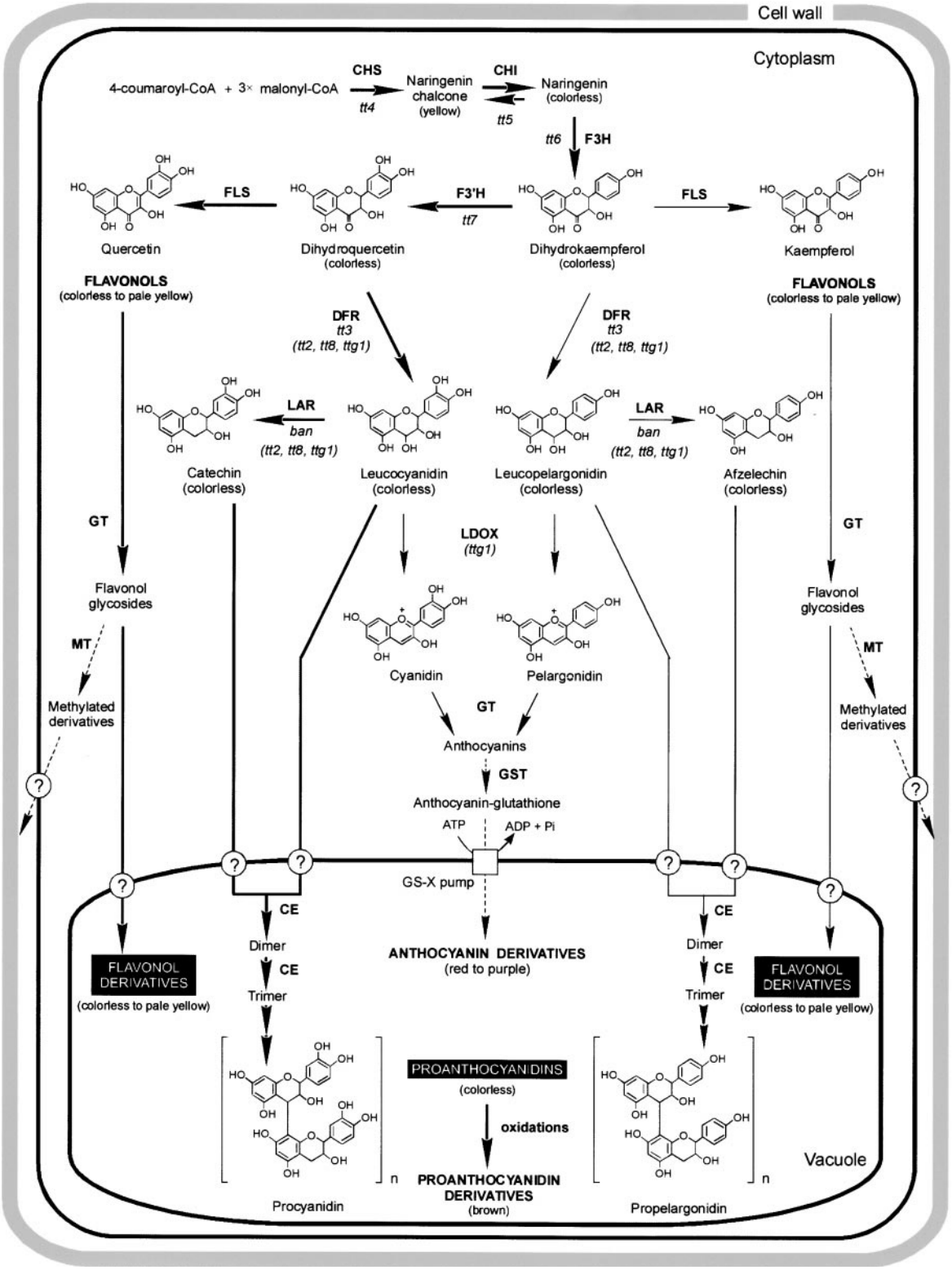

Figure 1. Scheme of the Flavonoid Biosynthetic Pathway.

The subpathway leading to the formation of flavonoid pigments in the Arabidopsis seed coat is indicated by boldface arrows; thin arrows repre-

and D.R. Smyth, personal communication) mutants, which encode a basic helix-loop-helix domain protein (Nesi et al., 2000), a WD40-repeat protein (Walker et al., 1999), and a WRKY family protein (C.J. Johnson and D.R. Smyth, personal communication), respectively. The remaining mutants—*tt1*, *tt2*, *tt9*, *tt10* (Shirley et al., 1995), *tt11*, *tt12*, *tt13*, *tt14* (Debeaujon et al., 2000), *tt15* (Focks et al., 1999), *tt16*, *tt17*, and *tt18* (Nesi et al., 2000)—have not been studied at the molecular level. In addition to testa pigmentation mutants, the *anthocyaninless* (*anl*) mutants *anl1* and *anl2* are affected in vegetative plant parts only. The *ANL2* gene encodes a homeodomain protein (Kubo et al., 1999).

The main flavonoids found in Arabidopsis seeds are PAs of the procyanidin type and derivatives of the flavonol quercetin, both of which are produced from dihydroquercetin (Chapple et al., 1994). At least three enzymes are involved in the conversion of leucocyanidins to catechin and procyanidins (Figure 1): (1) an NADPH-dependent reductase that converts leucocyanidin (flavan-3,4-diol) to catechin (flavan-3-ol), which probably corresponds to the BAN protein in Arabidopsis (Devic et al., 1999); (2) hypothetically, a condensing enzyme that adds leucocyanidin to catechin (initiating unit) to form a dimeric procyanidin (condensed tannin); and (3) a second condensing enzyme that adds leucocyanidin to the procyanidin dimer, leading to elongation of the polymers (Kristiansen, 1984). However, the fact that the immature testa of the *tt7 ban* double mutant (Albert et al., 1997) harbors a pelargonidin-like orange color suggests that the minor (pro)pelargonidin subpathway is also functional.

Flavonoids are assumed to play important functions, such as protecting against UV light damage, pathogen attack, and oxidative stress (Shirley, 1996; Grotewold et al., 1998). An increasing body of evidence suggests that these protective mechanisms also play a role in seed biology (Winkel-Shirley, 1998). For example, the toxicity of PAs to fungi, bacteria, and insects is well documented (Scalbert, 1991; Bell et al., 1992). Flavonoids such as quercetin and catechin are effective antioxidants (Rice-Evans et al., 1997) that might limit seed deterioration during storage. Moreover, PAs reduce water uptake and imbibition damage by solute leakage and may act as a mechanical barrier, preventing embryo injury (Halloin, 1982; Bell et al., 1992; Kantar et al., 1996). As a consequence of their action on testa hardening, these compounds play an indirect restrictive role in seed germination by hampering radicle protrusion from the integuments and therefore are important determinants of seed coat–imposed dormancy (Debeaujon et al., 2000). In terms of nutrition, seed flavonoids incorporated into the human diet may protect against cardiovascular diseases and certain cancers (Rice-Evans et al., 1997).

Flavonoids, particularly the hydrophobic aglycone forms, are toxic endogenous chemicals for the cell machinery because of their high chemical reactivity. Therefore, they need to be removed from the cytoplasm immediately after their synthesis. This can be done either by sequestration in the central vacuole, as for anthocyanins, PAs, phytoalexins, and flavonol glycosides, or by excretion into the cell wall, as described for polymethylated flavonol glucosides (Hrazdina, 1992; Ibrahim, 1992; Klein et al., 1996; Li et al., 1997; Grotewold et al., 1998). Vacuoles offer a larger storage space than cell walls, which is important for flavonoids to reach concentrations great enough to function in the protection against predators and pathogens or as UV light sunscreens or attractants (Klein et al., 2000). Typically, the detoxification process for flavonoids, which is also used by plants to detoxify xenobiotics such as pathogen toxins and agrochemicals (herbicides, pesticides), requires three phases. In phase I (activation), enzymes such as cytochrome P450 monooxygenases and hydrolases introduce or expose functional groups of the appropriate reactivity for phase II enzymes. During phase II (conjugation), the activated metabolite is deactivated by covalent linkage to an endogenous hydrophilic molecule such as glucose, malonate, glutathione, or glucuronate to form a water-soluble conjugate, the reaction being catalyzed by the corresponding transferase enzymes. Finally, in phase III (compartmentation), the inactive water-soluble conjugates are exported from the cytosol by membrane-located transporters (Sandermann, 1992; Coleman et al., 1997; Rea, 1999; Klein et al., 2000). In the *bronze-2* (*bz2*) mutant of maize, cyanidin-3-glucoside (C-3-G) accumulates in the cytosol, where it is oxidized to a brown pigment different from the typical purple C-3-G vacuolar form (Marrs et al., 1995). The *BZ2* gene encodes a type III glutathione *S*-transferase (GST) enzyme that was proposed to be involved in the conjugation of C-3-G with a glutathione (GSH) tag. This tripeptide would allow the vacuolar transfer of C-3-G by a glutathione *S*-conjugate (GS-X) pump (Marrs et al., 1995; Alfenito et al., 1998). The gene encoding

Figure 1. (continued).

sent an alternative subpathway that functions predominantly in Arabidopsis vegetative parts. The pathways to polymethylated flavonols (*Chrysosplenium*) and to anthocyanin vacuolar transport (maize) have not been found to occur in Arabidopsis and are thus hypothetical (dashed arrows). Enzymatic steps affected in *tt* mutants are indicated, with mutants corresponding to regulatory genes given in parentheses and the other mutants corresponding to structural genes. Enzymes are shown in boldface letters. CE, condensing enzyme; CHI, chalcone isomerase; CHS, chalcone synthase; DFR, dihydroflavonol-4-reductase; F3H, flavonol 3-hydroxylase; F3′H, flavonol 3′-hydroxylase; FLS, flavonol synthase; GST, glutathione *S*-transferase; GS-X, glutathione conjugate; GT, glycosyltransferase; LAR, leucoanthocyanidin reductase; LDOX, leucoanthocyanidin dioxygenase; MT, methyltransferase.

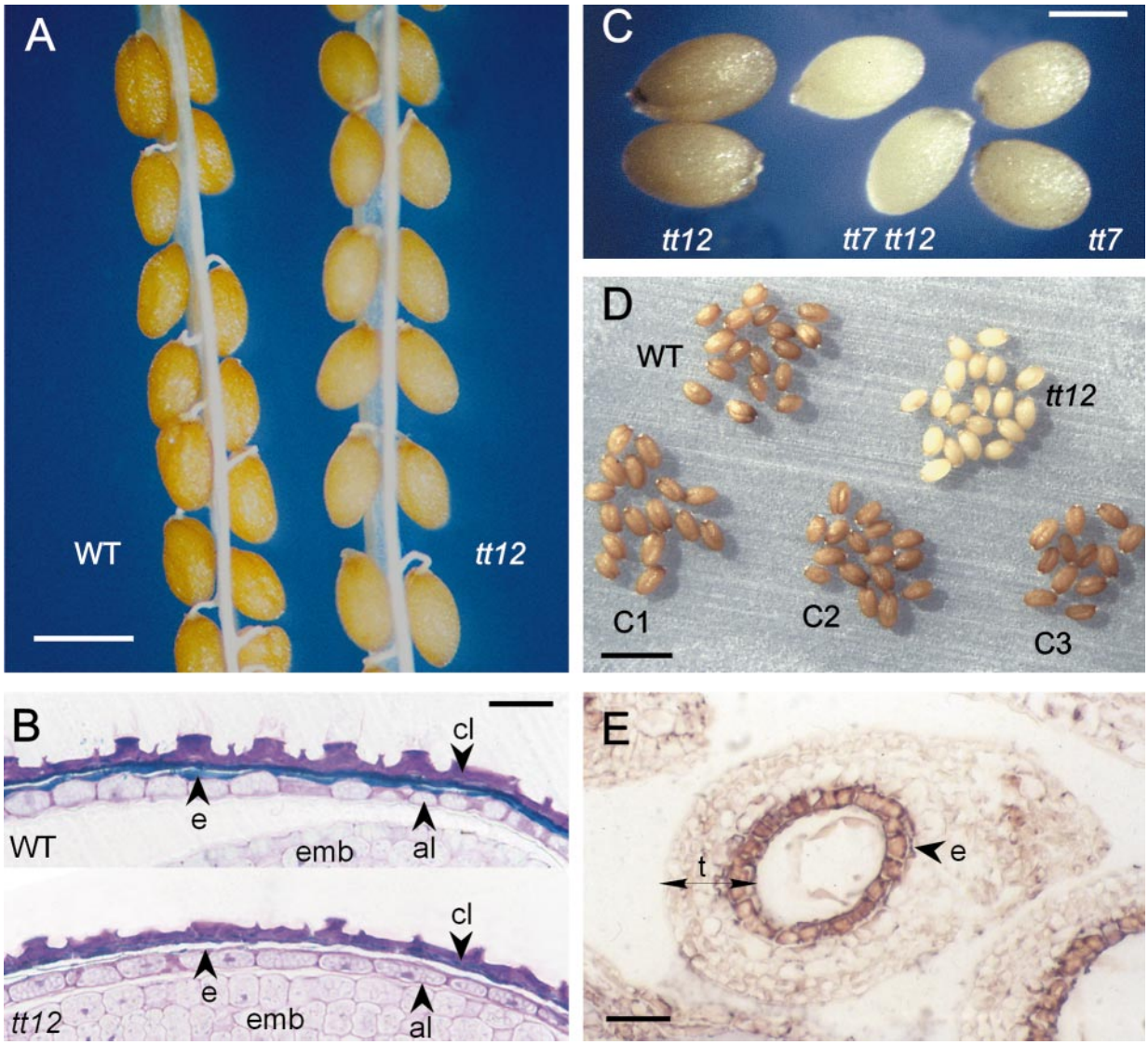

Figure 2. Seed Phenotypes.

Mature seed subtle color nuances (as they appear in **[A]**, **[C]**, and **[D]**) are likely to vary slightly with the conditions of plant culture, the age of seed lots, and photograph conditions. These conditions were kept identical for all genotypes within each photo but differ among photos, which limits the comparability of panels **(A)**, **(C)**, and **(D)**.

(A) Mature seeds of the wild-type (WT) and the *tt12* mutant. The *tt12* mutant seeds, which have lost the bright brown-orange color characterizing wild-type seeds, are dull pale brown. Bar = 250 μm.

(B) Cytochemical localization of polyphenolic compounds (in blue-green; arrowheads) in the testa of mature wild-type and *tt12* seeds after staining with toluidine blue O. al, aleurone layer; cl, four crushed parenchymatic layers of the testa; e, endothelium layer of the testa; emb, embryo. Bar = 40 μm.

(C) Mature seeds of the *tt7* and *tt12* single mutants, and of the *tt7 tt12* double mutant. Bar = 250 μm.

(D) Molecular complementation of the *tt12* mutation. Freshly harvested seed lots after ripening for 6 months in anoxia (under Scotch tape on a slide) are presented. The seeds of three independent complementing transformants (C1 to C3) show a wild-type brown color, unlike *tt12* seeds, which stayed very pale brown. Bar = 1 mm.

(E) Expression of the *TT12* gene in the endothelium layer of a wild-type immature seed at the globular stage of embryo development. The section was hybridized with a digoxigenin-labeled antisense *TT12* probe and observed with a light microscope. The signal is dark pink (arrowhead). e, endothelium layer of the testa; t, testa. Bar = 40 μm.

this pump has not been cloned. However, it is inferred from the vanadate sensitivity of the GS-X pump in planta that it may be similar to *Hs*MRP1 and *Sc*YCF1, the multidrug resistance ATP binding cassette (ABC) transporters from human and yeast, respectively (Rea, 1999). Two cloned Arabidopsis homologs of the *Hs*MRP1 transporter could realize the uptake of glutathionated C-3-G in vacuolar membrane–enriched vesicles of yeast (Lu et al., 1997, 1998). However, neither this function nor the vacuolar localization of the proteins was shown to occur in planta, and Arabidopsis mutants for these genes have not been described. Li et al. (1997) demonstrated that the isoflavonoid phytoalexin medicarpin conjugated to GSH was transported into vacuolar membrane vesicles from mung bean hypocotyls by a GS-X pump. Recent data showed that AN9, a BZ2 functional homolog of petunia (Alfenito et al., 1998), may be a flavonoid binding protein serving as a cytoplasmic flavonoid carrier protein rather than the GST triggering the formation of a flavonoid–glutathione conjugate (Mueller et al., 2000).

A new *tt* mutant of Arabidopsis isolated previously in our laboratory, *tt12*, was described briefly in physiological studies involving several other testa mutants (Debeaujon and Koornneef, 2000; Debeaujon et al., 2000). Here, we report the isolation and phenotypic characterization of this mutant, which is affected specifically in seed coat flavonoid pigmentation, together with the molecular cloning of the *TT12* gene by T-DNA tagging. The *TT12* gene is related to members of a new family of secondary transporters that Brown and coworkers (1999) termed the MATE (multidrug and toxic compound extrusion) family. This, together with cytological data, suggests that the TT12 protein may be required for the vacuolar transport of flavonoids.

RESULTS

Isolation and Genetic Analysis of a Seed Pigmentation Mutant

A collection of T-DNA transformants in the Wassilewskija-1 (Ws-1) genetic background (Feldmann, 1991) was screened for mutants exhibiting a reduced seed dormancy compared with wild-type seeds obtained under the same environmental conditions. Pool number CS2649 yielded a putative mutant whose only visible phenotype was in testa pigmentation. Seeds of this mutant were paler than their brown wild-type counterparts (Figure 2A), but vegetative parts synthesized purple anthocyanins normally (data not shown). Wild-type seeds placed in aerobic conditions generally darken with storage time. This darkening also occurred in *tt12* seeds, but to a far lesser extent. When freshly harvested wild-type and mutant seeds were placed in anoxia (under Scotch tape on a slide), darkening was observed only in wild-type seeds (Figure 2D).

Reciprocal crosses with wild-type plants revealed that the seed color mutation was maternally inherited. In an F2 population, 156 plants produced brown wild-type seeds and 44 plants formed pale brown mutant seeds, which fitted a 3:1 ratio of wild-type and mutant phenotypic classes ($\chi^2 = 0.96$; $P > 0.05$). Altogether, these data demonstrate that the seed color phenotype of the mutant results from a monogenic recessive mutation with maternal inheritance. The reduced dormancy trait of the *tt12* mutant was confirmed by a germination time-course experiment performed with freshly harvested seed lots (Figure 3). Reduced dormancy appeared to be maternally inherited, like the pale brown seed color phenotype.

Because the mutation was likely to affect flavonoid pigmentation of the testa, allelism tests were performed with the 11 *tt* mutants available at that time (Shirley et al., 1995). Complementation was observed in all cases. Therefore, the new mutant was named *tt12*. The novelty of the locus was further confirmed by linkage analyses using F2 and F3 segregation data from crosses with the chromosome 3 markers *long hypocotyl 2* (*hy2*), *glabra 1* (*gl1*), and *eceriferum 7* (*cer7*). This revealed a very tight linkage between *tt12* and *cer7*. The position of *tt12* relative to the neighboring *tt5* and *tt6* mutations was also determined by analyzing the linkage of *tt12* with the respective mutants. Genetic mapping data are summarized in Figure 4.

Histological Characterization of the *tt12* Mature Testa

The phenolic compounds deposited in the cells of the wild-type endothelium layer (blue-green after toluidine blue O staining)

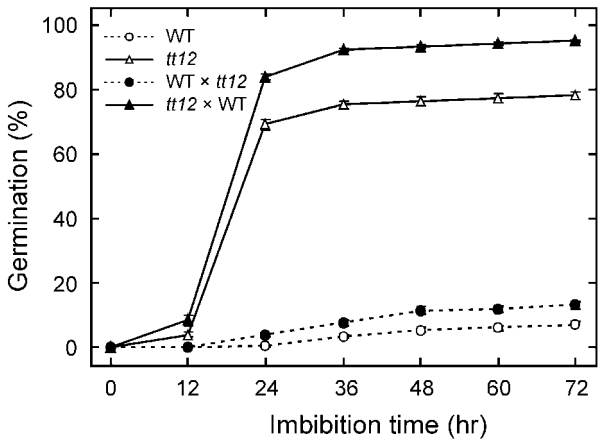

Figure 3. Genetic Determinism of the Reduced Dormancy Phenotype in the *tt12* Mutant.

The time course of germination for freshly harvested seeds (7 days of dry storage) is presented for the wild type (WT; Ws-1), *tt12*, and F1 progeny from reciprocal crosses. The parent mentioned first is the female parent.

were not detected in the *tt12* testa (Figure 2B) except as traces in the endothelium cell walls and in the crushed parenchymal layers above the endothelium. The *tt12* testa tissues also seemed less resistant to mechanical stress, because they were easily damaged during the process of microtome slicing. Scanning electron microscopic observation of the *tt12* seed surface revealed no abnormalities (data not shown).

Pattern of Pigment Accumulation in the Testa during Seed Development

PAs and their catechin and leucoanthocyanidin precursors are colorless compounds before being oxidized to brown products during seed maturation. Therefore, a colorimetric test is necessary to determine their presence or absence during early seed development (Jende-Strid, 1993). We used the vanillin assay to follow the timing and localization of PA accumulation in seeds of the wild type and *tt12* mutant during their development. In acidic conditions, vanillin (vanillaldehyde) condenses to flavan-3,4-diols (leucoanthocyanidins), flavan-3-ol monomers (catechins), and polymers (PAs) to give a cherry-red product. The red color is attenuated with the increasing degree of PA polymerization because condensation takes place at terminal units only (Deshpande et al., 1986).

In wild-type seeds, PA deposition was limited to the endothelium layer, which is the innermost layer of the testa. It was not detected before the two-cell stage of embryo development (Figure 5A) and appeared first in the micropylar area (arrowheads) before spreading all over the testa. The site of intracellular localization was the vacuole. PA precursors quickly accumulated until complete filling of the large endothelium cells, which occurred approximately at the heart stage of embryo development (Figures 5C and 5E). At this stage, the characteristic chalazal bulb was completely pigmented (Figure 5E). From the early torpedo stage onward, endothelial pigmentation became denser and the color darkened from cherry-red to brown-red (Figure 5G). Around the late torpedo–early walking stick stage, a second, yellow pigment appeared in the three parenchymal layers above the endothelium, the color of which indicated that this pigment differed from PAs (Figures 5I and 5K). In the absence of vanillin, this pigment had a pale brown color that darkened with time and appeared first in the endothelium layer before spreading to the three parenchymal layers (data not shown).

Lower levels of PAs and precursors accumulated in vacuoles of the *tt12* mutant (Figures 5B, 5D, 5F, and 5H). The diffuse pigmentation pattern suggested that a substantial portion of the pigments may have accumulated in the cytoplasm as well. The visible brown pigment also was detected, although it was present in reduced amounts, had a slightly duller color, and was spread more diffusely in testa layers (Figures 5J and 5L). Another striking difference with the wild type was the absence of pigmentation at the chalazal bulb (Figure 5L, arrowhead). However, the timing of appearance and the tissue distribution of pigments did not differ from what was observed in wild-type seeds.

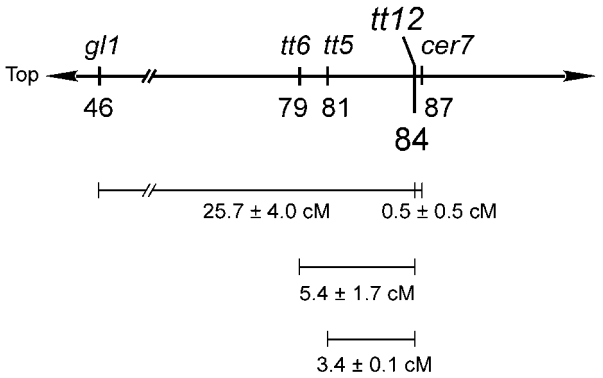

Figure 4. Localization of the *tt12* Mutation on the Genetic Map of Chromosome 3.

The genomic region corresponds to the bottom of chromosome 3, with "Top" indicating chromosome orientation. The genetic distance in centimorgans (cM) between two mapped markers is indicated below the given interval, plus or minus the standard error. The map is anchored by the *gl1* marker position (Koornneef, 1994). The other marker positions are deduced from our own linkage data combined with the genetic map described by Koornneef (1994). The position of *tt6* to the left of *tt5* was deduced from the molecular mapping data of Camilleri et al. (1998).

Double Mutant Analysis

To understand the relationship of *TT12* to other genes involved in testa flavonoid metabolism, we studied the interaction between *tt12* and other recessive mutations affecting testa pigmentation. The color of mature seeds from single and double mutants was observed before and after vanillin staining to detect PAs, with a distinction being made between the chalazal area and the rest of the seed (seed body) (Table 1). With respect to the seed body, the *tt12* mutation was epistatic to *tt9*, *tt10*, *tt13*, and *tt14*. On the other hand, the *tt2*, *tt4*, *tt5*, *tt6*, *tt8*, and *tt11* mutants were epistatic to *tt12*. An important point was that *tt7 tt12* double mutant seeds were yellow, unlike the seeds of both parents, which were very pale brown and dull pale brown, respectively (Figure 2C). The vanillin test indicated that *tt7 tt12* mature seeds lack PAs. Other double mutants with a novel phenotype were *ban tt12*, which resembled *ban* seeds but with a paler and less green appearance, and *tt15 tt12*, which was pale orange-brown, in contrast to the grayish pale brown and dull pale brown parental seeds. The double mutants of *tt1*, *tt3*, and *ttg1* with *tt12* looked like the first parent but with a dull appearance. In a *tt12* background, 10 of 16 pigmentation

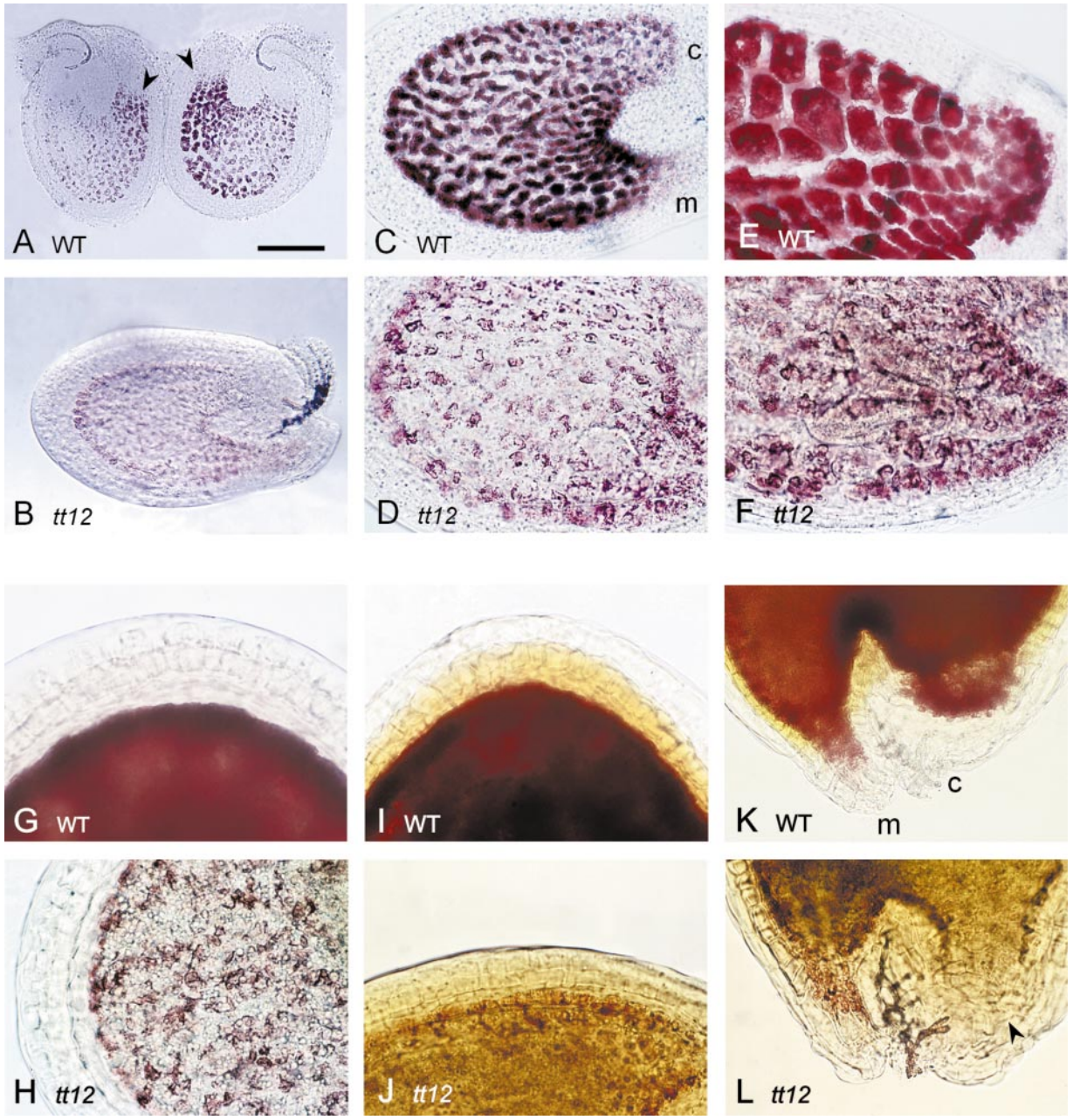

Figure 5. Proanthocyanidin Pigment Deposition in Developing Seeds of the Wild Type and the *tt12* Mutant Analyzed with Vanillin Staining.

Immature seeds were incubated on a slide in vanillin HCl before observation with a microscope. Ovules and seeds younger than the two-cell stage of embryo development are not shown because no pigment was detected. The wild-type seeds (upper photo lines) are compared with *tt12* mutant seeds at the same developing stage (lower photo lines).

(A) and **(B)** Developing wild-type seeds at approximately the four-cell stage of embryo development (ED). PAs and precursors appear dark red. Arrowheads indicate the micropylar areas where pigment was first localized before spreading over the entire endothelium layer. **(B)** Corresponding stage in *tt12*.

(C) and **(D)** Wild-type seed at the late globular stage of ED. The endothelium layer is completely pigmented, which allows distinction of the micropyle from the chalaza, but vacuoles are not completely filled up. **(D)** Corresponding stage in *tt12*.

(E) and **(F)** Wild-type seed at the heart stage of ED. The chalazal bulb shows large endothelial cells filled with pigments. **(F)** Corresponding stage in *tt12*.

(G) and **(H)** Wild-type seed at the torpedo stage of ED. **(H)** Corresponding stage in *tt12*.

(I) through **(L)** Wild-type seed at the walking stick–cotyledonary stage of ED. A second pigment is spreading from the endothelium layer to the upper parenchymal cell layers. **(I)** and **(K)** show the seed region opposite the chalaza–micropyle pole and the chalaza–micropyle areas, respectively. **(J)** and **(L)** Corresponding stages in *tt12*.

c, chalaza; m, micropyle; WT, wild type. Bar in **(A)** = 75 μm for **(A)**, 60 μm for **(B)**, 50 μm for **(C)**, and 30 μm for **(D)** to **(L)**.

Table 1. Phenotypic Characterization of Double Mutants between *tt12* and Other Pigmentation Mutants

Single Mutant				Double Mutant			
Locus	Seed Body	Chalaza	Vanillin[a]	Loci	Seed Body	Chalaza	Vanillin[a]
tt1-1	Golden yellow	Brown	−/+	*tt1-1 tt12-1*	Dull *tt1-1*	Pale gray	−/−
tt2-1	Golden yellow	None	−/−	*tt2-1 tt12-1*	*tt12-2*	None	−/−
tt3-1	Grayish yellow	Pale gray	−/−	*tt3-1 tt12-1*	Dull *tt3-1*	Gray	−/−
tt4-1	Pale yellow	None	−/−	*tt4-1 tt12-1*	*tt4-1*	None	−/−
tt5-1	Lemon yellow	Pale gray	−/−	*tt5-1 tt12-1*	*tt5-1*	None	−/−
tt6-1[b]	Very pale brown	Pale brown	−/−	*tt6-1 tt12-1*	*tt6-1*	Brown	−/−
tt7-1[b]	Very pale brown	Pale brown	−/−	*tt7-1 tt12-1*	Yellow	Gray	−/−
tt8-1	Lemon yellow	None	−/−	*tt8-1 tt12-1*	*tt8-1*	None	−/−
tt9-1	Grayish beige	Black[c]	−/+	*tt9-1 tt12-1*	*tt12-1*	Dark brown	−/−
tt10-1[d]	Pale brown	Brown[c]	+/+	*tt10-1 tt12-1*[e]	*tt12-1*	Pale brown	−/−
tt11-2	Pale brown	Pale brown	−/−	*tt11-2 tt12-1*	*tt11-1*	Pale brown	−/−
tt13-1	Pale brown	Dark brown	−/+	*tt13-1 tt12-1*	*tt12-1*	Dark brown	−/−
tt14-1[d]	Pale brown	Dark brown	+/+	*tt14-1 tt12-1*[e]	*tt12-1*	Dark brown	−/−
tt15-1	Grayish pale brown	Black[c]	−/+	*tt15-1 tt12-1*	Pale brown	Dark brown	−/−
ttg1-1	Lemon yellow	None	−/−	*ttg1-1 tt12-1*	Dull *ttg1-1*	None	−/−
ban-2	Grayish green	Black[c]	−/+	*ban-2 tt12-1*[c]	Pale *ban*	Dark brown	−/−
Ws-1	Brown	Dark brown	+/+				
tt12-1	Dull pale brown	Pale brown	−/−				

[a] Proanthocyanidin detection with vanillin treatment: seed body (whole seed except chalazal area)/chalazal area; +, presence of red pigments; −, absence of red pigments.

[b] Mature *tt7* seeds and to a lesser extent *tt6* seeds are slightly spotted.

[c] The dark pigmentation of the chalazal area is more extended than with the other genotypes, and seeds appear spotted around this area for *tt9*, *ban*, *tt15,* and *ban tt12*.

[d] The mutants are pale brown at harvest and darken during after-ripening until they are nearly identical to wild-type Ws-1 seeds.

[e] Both *tt10 tt12* and *tt14 tt12* darken very little with time, like *tt12* but unlike *tt10* and *tt14*.

mutants showed modified chalazal color. Interestingly, the black chalaza of *tt15* and *ban* switched to dark brown. Moreover, the spotted appearance that is characteristic of these single mutants was conserved in double mutants. In the other double mutants, the chalaza color became paler (*tt10* and *tt11*), grayer (*tt1*, *tt3*, and *tt7*), or even disappeared (*tt5* and *tt8*). The vanillin test on mature seeds revealed that the *tt12* mutation systematically led to a complete disappearance of PAs in all of the mutants that synthesized it.

Molecular Cloning of the *TT12* Gene

The F2 progeny from a cross between the wild type and the *tt12* mutant were analyzed for both kanamycin resistance conferred by the T-DNA (Feldmann, 1992) and seed color. The *tt12* line segregated for only one functional kanamycin resistance locus in a Mendelian fashion (3:1 ratio of resistant to sensitive plants). None of the 44 F2 plants with a *tt12* phenotype (pale brown seeds) was sensitive to kanamycin or segregated for this trait. Therefore, the data support the hypothesis that the T-DNA and the *tt12* mutation were tightly linked. DNA gel blot analysis of the *tt12* mutant with probes corresponding to different parts of the T-DNA revealed the presence of only one complete T-DNA unit with inverted tandem repeats of truncated T-DNAs at both borders (data not shown). Together, the genetic and molecular analyses strongly suggest that the *TT12* gene was tagged by the T-DNA, thereby allowing its molecular cloning. The T-DNA used to generate the mutant population contains the origin of replication and the ampicillin resistance gene of plasmid pBR322, which enable the recovery of T-DNA–plant DNA junction fragments as plasmids in *Escherichia coli* by plasmid rescue (Feldmann, 1992). A 13.5-kb plasmid (pEB8) containing 2.2 kb of plant DNA flanking the right border of the T-DNA was isolated. Using a polymerase chain reaction (PCR) primer pair designed from the rescued flanking DNA and PCR screening of the CIC yeast activation chromosome library, we localized this genomic region on yeast activation chromosome CIC11A1 anchored by the pCIT1210 and m339 markers at the bottom of chromosome 3 (Camilleri et al., 1998). The molecular mapping data for *tt12* thus confirmed the genetic mapping using morphological markers (Figure 4). The rescued plant DNA was used to identify a 15-kb genomic λ clone spanning the site of T-DNA insertion (Figure 6A). A 4.5-kb EcoRI-KpnI genomic fragment was sequenced on both strands. A BLASTN search with this sequence in the GenBank database did not yield any ex-

pressed sequence tag. Using the 5′ part of the genomic clone to the KpnI site as a probe to screen a silique cDNA library, we recovered a full-length cDNA spanning the site of T-DNA insertion (Figure 6A). When used as a probe in DNA gel blot analyses, this cDNA clone detected a restriction fragment length polymorphism between genomic DNAs from wild-type and *tt12* plants (Figure 6C). To provide functional proof that the genomic area spanned by the cDNA corresponded to the *TT12* gene, we retransformed kanamycin-resistant *tt12* mutant plants (T0) with a T-DNA harboring the 4.5-kb EcoRI-KpnI genomic fragment (Figure 6A) and a hygromycin resistance gene as a selectable marker that can be used in kanamycin-resistant plants. Three independent primary transformants (T1) were recovered on the basis of their resistance to both kanamycin and hygromycin. All of them produced wild-type brown seeds (Figure 2D). The progeny from selfing of the complementing transformant C1 containing one functional hygromycin resistance gene were analyzed further (Table 2). T2 plants segregated for both seed color and hygromycin resistance. The T-DNA insert and the *tt12* mutation segregated independently, with a 3:1 ratio of hygromycin-resistant to hygromycin-sensitive plants and brown to pale brown seeds. Only hygromycin-resistant plants produced wild-type brown seeds. Together, these data demonstrate that the introduced genomic fragment was able to complement the *tt12* mutation and therefore contains the *TT12* gene. After we mapped, cloned, and sequenced the *TT12* gene, it could be localized on bacterial artificial chromosome F17J16 (gene 80; GenBank accession number CAB86931) when this sequence was released in databases.

Structure of the *TT12* Gene and Sequence Analysis of the Deduced Protein

The *TT12* cDNA was sequenced on both strands and aligned to the 4.5-kb EcoRI-KpnI genomic fragment. The *TT12* gene, with its eight exons and seven introns, spanned 2261 bp of genomic DNA (Figure 6B). Exons ranged from 57 to 545 bp, and introns ranged from 70 to 160 bp. The 36-bp 5′ untranslated region was not preceded by a stop codon in frame to the first ATG. The context of this ATG, CGGACCaugA, resembled the consensus sequence GCCACCaugG proposed by Kozak (1999) for eukaryotic functional ATG codons. Moreover, a CAAT box and a TATA box were found at −102 and −27 bp, respectively, from the transcription initiation site. No typical poly(A) signal was found in the 61-bp 3′ untranslated end. The T-DNA insertion site was localized at the beginning of the first intron (Figure 6B). The 1621-bp *TT12* cDNA contained a single open reading frame coding for a putative polypeptide of 507 amino acid residues with a predicted molecular mass of 55.1 kD and a calculated pI of 8.3. Hydropathy analysis according to Kyte and Doolittle (1982) (Figure 6D) predicted that the TT12 protein contained 12 putative transmembrane segments (TMs) connected by

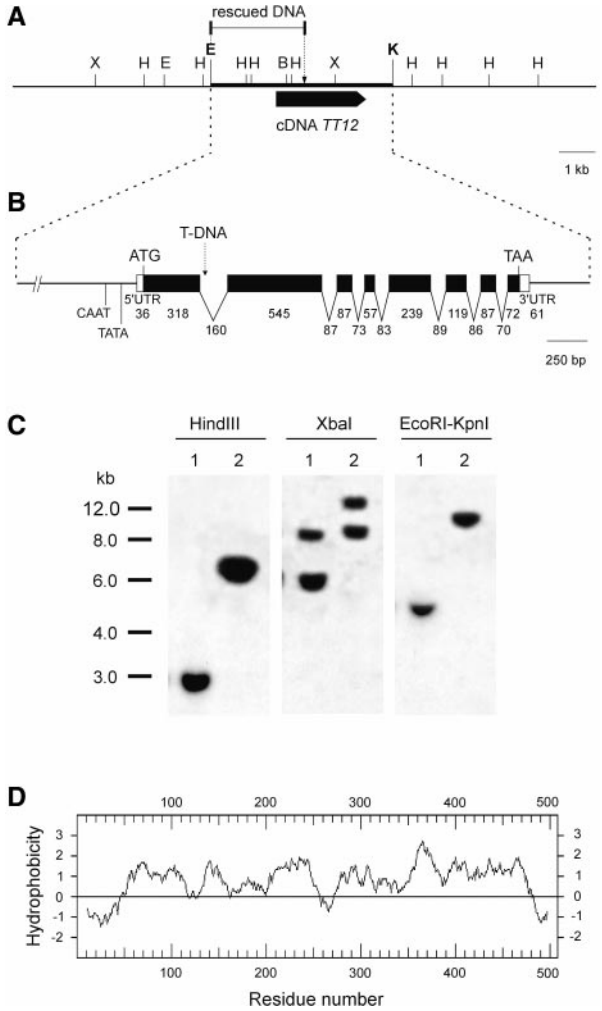

Figure 6. Organization of the Genomic Region and Structure of the *TT12* Gene.

(A) Localization of *TT12* cDNA on the restriction map of a λ clone. The arrow indicates the sense of transcription. The genomic DNA fragment isolated by plasmid rescue is shown. The genomic fragment used to complement the *tt12* mutation is indicated by a thick line. Restriction sites are as follows: B, BamHI; E, EcoRI; H, HindIII; K, KpnI; and X, XbaI.

(B) Sequence features of the *TT12* gene. Boxes represent exons, with white boxes indicating the cDNA untranslated regions (UTRs). The arrow indicates the site of T-DNA insertion in the *tt12* mutant. Sizes are drawn to scale. The entire *TT12* cDNA sequence was submitted to GenBank under the accession number AJ294464.

(C) DNA gel blot analysis of wild-type and *tt12* plants. Restricted genomic DNA of wild-type (lanes 1) and *tt12* (lanes 2) plants probed with the complete cDNA reveals a polymorphism between wild type and *tt12*. The positions and lengths (in kilobases) of DNA molecular mass markers are indicated at left.

(D) Hydropathy profile of the TT12 protein, as determined by the method of Kyte and Doolittle (1982), using a window of 19 amino acid residues.

Table 2. Complementation of the *tt12* Mutant Phenotype in the T3 Generation of Transformant C1

	Hygromycin[b]			
T3 Seed Color[a]	R	H	S	Total
Brown	18	52	0	70
Pale brown	0	0	18	18
Total	18	52	18	88

[a] Brown, wild-type seed color; pale brown, mutant seed color. The observed segregation for seed color is in agreement with a 3:1 ratio ($\chi^2 = 0.97$; $P > 0.05$), indicating monogenic inheritance.

[b] Genotype of T2 plants from transformant C1 deduced from the behavior of T3 seedlings on hygromycin: R, homozygous resistant; H, heterozygous; S, sensitive. The observed segregation for hygromycin resistance is in agreement with a 1:2:1 ratio ($\chi^2 = 2.91$; $P > 0.05$), indicating monogenic inheritance. All T2 plants were homozygous for kanamycin resistance.

hydrophilic loops of various sizes. The prediction of transmembrane domains using the transmembrane hidden Markov model (TMHMM) program (http://genome.cbs.dtu.dk/services/TMHMM/) suggested that the N and C hydrophilic termini were located inside the cellular compartment. This membrane topology is characteristic of many transporter proteins found in both prokaryotes and eukaryotes (Henderson, 1993). A comparison of the predicted TT12 protein with sequences in various databases was performed with the Gapped BLASTP server, yielding representatives from all three kingdoms of life. The best global similarities were found with 30 Arabidopsis proteins of unknown function, among which F8K4.9 gave the highest score (46% identity and 64% similarity on a 442–amino acid stretch covering the TT12 sequence from TM1 onward, with no gap). The F9L1.10 protein exhibits 33% identity and 50% similarity on a 435–amino acid stretch with TT12 (see Results for information on the other proteins). All of the proteins similar to TT12 ranged in length from 425 to 746 residues, with the exception of the Arabidopsis protein T8O5.110, which had 1094 amino acids. According to the TMHMM program, the number of TMs of paralogous proteins varies between eight and 13. However, these data are only predictions based on computer analysis of protein sequences and therefore must be considered cautiously. The other *TT12*-related eukaryotic sequences were an expressed sequence tag from human, three genes from *Schizosaccharomyces pombe*, and two genes from *Saccharomyces cerevisiae*. The remaining sequences were all prokaryotic, from cyanobacteria, eubacteria (Gram positive and Gram negative), or archaebacteria. The *TT12* gene is related to those encoding the Erc1 (ethionine resistance conferring 1) protein from *S. cerevisiae*, which corresponds to the YHR032w open reading frame (26% identity and 45% similarity on a 411–amino acid stretch), the NorM (norfloxacin resistance M) protein from *Vibrio parahaemolyticus* (21% identity and 40% similarity on a 427–amino acid stretch), and the DinF (damage-inducible F) protein of *E. coli* (24% identity and 40% similarity on a 189–amino acid stretch) (Kenyon and Walker, 1980; Shiomi et al., 1991; Morita et al., 1998). The Erc1, NorM, and DinF proteins are carrier-type transporters belonging to the MATE family and the only proteins of the family that have been characterized (Brown et al., 1999; Saier, 2000). A PSI-BLAST search with TT12 revealed a possible relationship with some members of the polysaccharide transporter family (an *O*-antigen transporter and a succinoglycan transporter from *Methanobacterium thermoautotrophicum* and a polysaccharide biosynthesis transporter from *Pyrococcus abyssi*).

An alignment of the sequence of TT12 with those of Erc1, NorM, DinF, and two closely related Arabidopsis protein sequences is shown in Figure 7. The F8K4.9, F9L1.10, Erc1, NorM, and DinF proteins were predicted to have 12, 11, 10, 12, and 13 TMs, respectively (TMHMM program). The hydropathy profiles of the six proteins were similar except in the area between TM8 and TM11, DinF having an additional TM in the N-terminal part. The region of greatest overall homology extended from the end of the hydrophylic N terminus to the beginning of the hydrophilic C terminus. Five domains (D1 to D5) appeared to be particularly conserved: D1 and D3 were both in internal hydrophilic loops (I1 and I4, respectively), and D3, D4, and D5 were located in TMs (TM7, TM10, and TM11, respectively) when referring to TT12 topology. Interestingly, a part of D1 (QAYGA motif) was also present in D3 in the DinF protein. Intramembranous charged residues often have essential functions (Paulsen et al., 1996). In this respect, it is important to note the presence of six charged residues in the TT12 TMs (Figure 7), among which only the E of TM7 was very conserved. The P in TM1 was present in all proteins except TT12, in which it was replaced by an A.

Expression of the *TT12* Gene

The pattern of *TT12* mRNA accumulation in various wild-type vegetative and reproductive tissues was determined using the *TT12* cDNA as a probe on blots of quantitative reverse transcription (RT)–PCR reactions performed for 18, 21, and 24 cycles (Figure 8A). The 1.6-kb RNA was detected only in reproductive tissues, from buds to siliques at the late heart–torpedo stage of embryo development (~6 to 7 days after pollination under our growth conditions), with a peak in siliques at the early globular–globular stage (~3 days after pollination). In contrast, *TT12* mRNA was completely absent from *tt12* siliques at the globular stage (Figure 8B), indicating that this T-DNA allele was null. All of the negative results were confirmed by 35-cycle PCR on the same RT samples (data not shown). This pattern of expression is consistent with the *TT12* cDNA being found in a silique library.

To define precisely the spatial pattern of *TT12* gene expression, in situ localization of the mRNA was performed using digoxigenin-labeled riboprobes. Hybridization with the

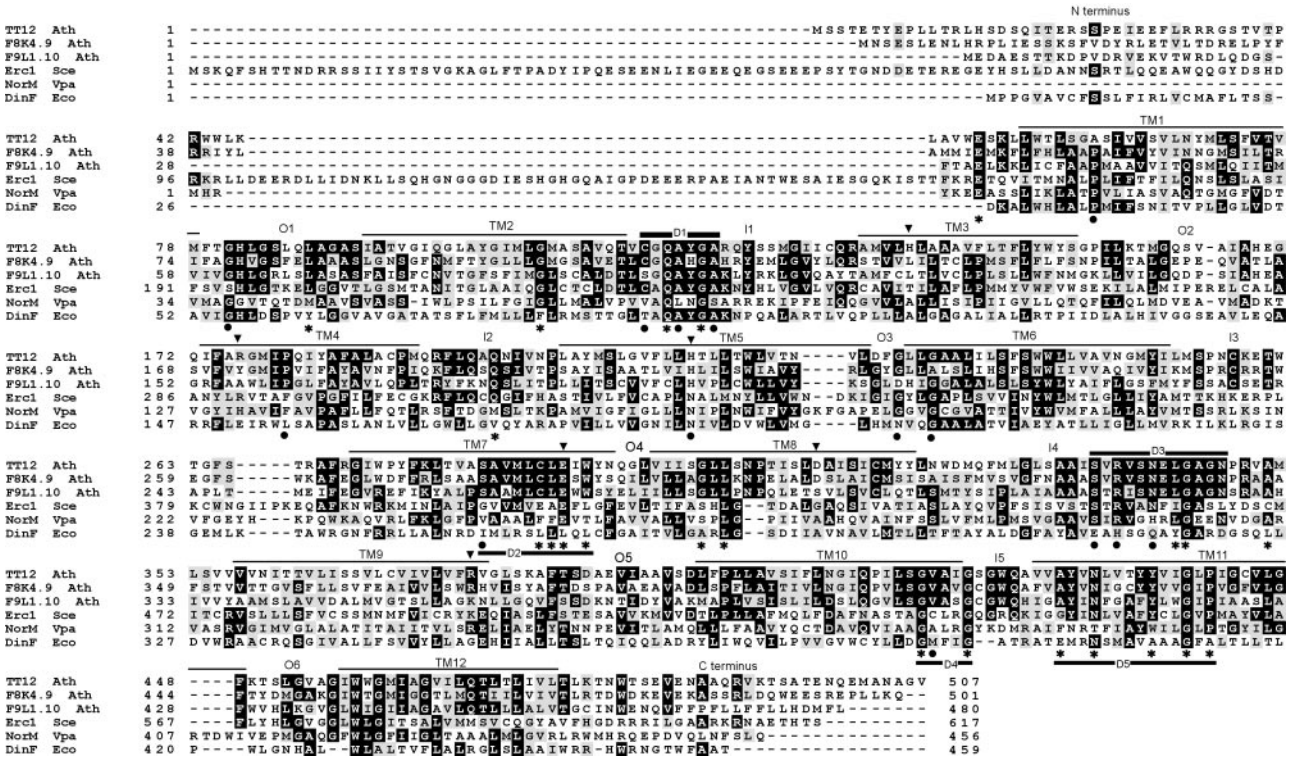

Figure 7. Alignment of TT12 with Five Related Proteins.

The alignment involves two close paralogs of TT12 and the three orthologous proteins from the MATE family that were previoulsy characterized. The six sequences were aligned using the CLUSTALW program with default parameters. Identical and similar residues are shown on backgrounds of black and gray, respectively. Gaps required for optimal alignment are indicated by dashes. The putative TMs of the TT12 protein, as determined by the TMHMM program, are delimited by thin lines above the sequences; outer (O) and inner (I) hydrophilic internal segments also are indicated. A comparison of TT12 with its 30 Arabidopsis paralogs was performed (data not shown); residues conserved in all sequences are indicated by stars, and those conserved in all but one sequence are indicated by dots. Triangles indicate the charged residues present in TMs. Conserved protein domains (D1 to D5) are represented by thick lines. Ath, Arabidopsis; Sce, *S. cerevisiae*; Vpa, *V. parahaemolyticus*; Eco, *E. coli*.

antisense probe appeared as a dark-pink precipitate. Figure 2E shows that the expression detected in a seed at the globular stage of development was restricted to the endothelium layer of the seed coat. Hybridization with a sense strand did not reveal any signal (data not shown).

DISCUSSION

The *tt12* Mutant Affected in Seed Coat Flavonoid Pigmentation Is Also a Reduced Seed Dormancy Mutant

The identification of seed color mutants on the basis of visual screening is convenient for the recovery of pale categories (pale yellow to very pale brown). However, mutants harboring more subtle color differences are easily missed. This explains why the pale brown to grayish brown classes are underrepresented in the Arabidopsis mutant collections (Debeaujon et al., 2000). Seeds weakened in testa structure or pigmentation exhibit reduced seed dormancy as a pleiotropic effect (Debeaujon et al., 2000). On the basis of this observation, we isolated a novel pale brown *tt* mutant, *tt12*, as a germinating individual among nongerminating freshly harvested seeds. The very mild color difference between *tt12* and wild-type seeds would have complicated the recovery of such a mutant by a visual screen. Both dormancy and color phenotypes were maternally inherited, as expected from characteristics of the testa that derives developmentally from ovule integuments. Histological analysis of the mature *tt12* testa revealed that the endothelium layer was deprived of phenolic compounds. This observation strongly suggested a defect in the biosynthesis or in the deposition of PAs, because these flavonoid pigments are known to accumulate in the endothelium (Albert et al., 1997; Debeaujon et al., 2000). The vanillin assay confirmed this suggestion. The polymeric nature of PAs and their ability to bind proteins probably explain the impermeabilizing and

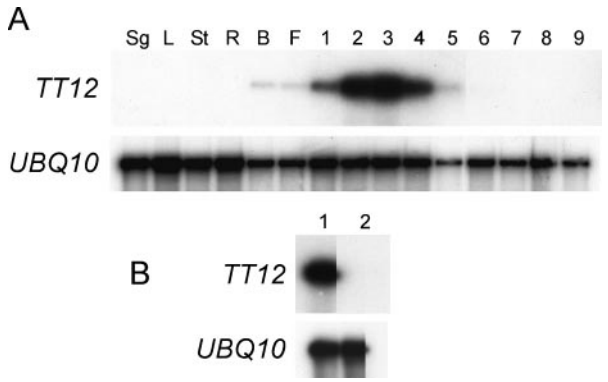

Figure 8. Detection of the *TT12* mRNA by Quantitative RT-PCR.

Results of 21-cycle PCR amplifications are presented. The Arabidopsis polyubiquitin gene *UBQ10* was used as a loading control.
(A) Detection in diverse tissues from wild-type plants. RNA preparations were made from 4-day-old seedlings (Sg), rosette leaves (L), stems (St), roots (R), buds (B), flowers (F), and immature siliques (stages 1 to 9; see Methods for descriptions).
(B) Detection in immature siliques (stage 3) of wild-type (lane 1) and *tt12* (lane 2) plants.

cell-cementing properties of these phenolic compounds and therefore their contribution to the germination-restrictive action of the testa.

PA Deposition in Vacuoles of the Endothelium Is Disturbed in *tt12*

The vacuolar deposition of PAs in the Arabidopsis endothelium is evident from the observation of wild-type immature seeds, in which the cell lumen progressively filled up with pigments during development. This pattern of pigment deposition is similar to that observed by Skadhauge et al. (1997) in immature seed coats of alfalfa stained with vanillin. Vanillin staining revealed a strong reduction of PA deposition in the vacuoles of *tt12* endothelial cells. Consequently, the contours of the vacuole were no longer visible, and the few remaining pigments seemed to be distributed randomly in the cytoplasm. The interpretation of Figures 5D and 5F is complicated by the fact that, under the vanillin assay conditions, PAs form aggregates and are not homogeneously soluble in aqueous solutions, as is the case for anthocyanins in *bz2* cells (Marrs et al., 1995). However if the problem were only a reduction of PAs in vacuoles, then the situation would be like the one observed in Figure 5A, in which young wild-type endothelium cells are not yet filled with PAs. The difference is that in the seeds shown in Figure 5A, pigment location is clearly delimited by the vacuole. The comparison of Figures 5A and 5B is informative on this point. The blue traces detected on the endothelium cell wall and the crushed cell layers of mature seeds after toluidine blue staining result either from the few PAs that were present in immature seeds or from other phenolic compounds that were not modified in *tt12*.

The pigmentation of wild-type endothelium is a two-step process. The deposition of colorless PAs (dark red in vanillin), ending with the vacuolar filling around the heart stage of embryo development, is followed by the appearance of visible brown pigment (yellow after vanillin staining) in the endothelium layer around the late torpedo–early walking stick stage. The flavonoid origin of this latter pigment is ascertained by the fact that it is absent in *tt4* mutant seeds (data not shown). With time, it spreads through the three parenchymal layers situated above the endothelium and becomes dark brown in mature wild-type seeds. It is a general observation that PAs isolated from seed coat or bark, or PAs allowed to "age," are colored, whereas PAs from fresh tissue are colorless. When exposed to oxygen, these phenolic compounds are susceptible to oxidation, leading to yellow-to-brown products such as quinone derivatives (Barz, 1977; Porter, 1992). The reaction has been reported to be catalyzed by oxidoreductase enzymes such as catechol oxidase, which is a polyphenoloxidase (Marbach and Mayer, 1975), and peroxidase (Egley et al., 1983; Bell et al., 1992). Baur and Walkinshaw (1974) reported that PAs were deleterious when they occupied a major portion of the cell, leading to exposure of the vacuolar content to air oxygen and oxidizing enzymes present in the cell. Therefore, it is likely that the brown pigment observed in Arabidopsis seeds is a product of PA oxidation. Its formation may occur after the breakdown of endothelial cells and subsequent interaction between vacuolar phenolic compounds and oxidoreductases. Later, the pigment may diffuse into the upper parenchymal cell layers. In *tt12* seeds, a reduction of PA accumulation may lead to limited formation of the brown flavonoid pigment, explaining the phenotype of the *tt12* mutant.

A striking difference between the wild type and the *tt12* mutant revealed by vanillin staining is the absence of chalazal bulb pigmentation in mutant seeds. This protuberance delineates the site of the chalazal endosperm described by Mansfield and Briarty (1994). Visibly, flavonoid metabolism in the chalazal area of the endothelium differs from that prevailing in the seed body, which also is suggested by the observation that body and chalaza pigmentations of other *tt* mutant and double mutant seeds seem to be under different genetic controls. This is related to what is observed in soybean (Todd and Vodkin, 1993) and *Brassica campestris* (Schwetka, 1982) seeds, in which one gene was found to determine hilum color specifically.

Interaction between *TT12* and Other Genes Involved in Seed Pigmentation

The relationship of *TT12* with 16 genes of the flavonoid pathway for which mutants are known (Figure 1) was estab-

lished by analysis of seed body color and vanillin assay in double mutants. The fact that early flavonoid biosynthetic mutants such as *tt4* are epistatic to *tt12* indicates that the function of TT12 depends on flavonoid biosynthesis. The epistasis of *tt12* to *tt9*, *tt10*, *tt13*, and *tt14* suggests that the latter corresponding genes exert their function after TT12. The interpretation of the results obtained with *tt1*, *tt9*, *tt10*, *tt11*, *tt13*, *tt14*, and *tt15* is complicated by the fact that their biochemical defects are still unknown. The additive effect of *tt7* and *tt12* is of interest because it suggests that *tt7* and *tt12* reduce the amount of PAs present in the mature testa by different mechanisms.

The TT12 Protein Resembles Multidrug Secondary Transporters

On the basis of its amino acid sequence, TT12 shows significant similarity with prokaryotic and eukaryotic members of the MATE family of 12-transmembrane helix transporters, such as NorM, DinF, and Erc1. Brown et al. (1999) did not propose any significant signature motifs for the new MATE family. However on the basis of a multiple sequence alignment of NorM with representative orthologs, they inferred that the most conserved regions were from mid TM5 to mid TM6 and the entire hydrophilic stretch between TM8 and TM9 comprising the D3 domain, when we consider the TT12 topology as a reference. Based on our multiple alignment, we propose that the domains D1, D2, D4, and D5 are also regions representative of the MATE family.

Previously, four families of transporters had been described that contain multidrug efflux systems: the major facilitator superfamily, the small multidrug resistance family, the resistance/nodulation/cell division family, and the ABC superfamily (Paulsen et al., 1996; Bolhuis et al., 1997). The recent definition of a fifth class, the MATE family, is considered an important finding in the field of multidrug efflux research (Brown et al., 1999). The major facilitator superfamily, small multidrug resistance, and resistance/nodulation/cell division families contain secondary transporters energized by the proton motive force, and the ABC superfamily consists of ATP-dependent primary transporters (Paulsen et al., 1996; Bolhuis et al., 1997). The NorM multidrug resistance protein from the Gram-negative bacterium *V. parahaemolyticus* mediates resistance to hydrophilic fluoroquinolone antibiotics such as norfloxacin and, to a lesser extent, to a range of cationic dyes and aminoglycosides but not to hydrophobic fluoroquinolones (Morita et al., 1998). The energization is probably due to a drug/H^+ antiport extrusion mechanism (Morita et al., 1998). The *Erc1* gene was reported to confer resistance to the toxic methionine analog ethionine and, when present in multiple copies, to direct the overaccumulation of *S*-adenosylmethionine in vacuoles of yeast cells (Shiomi et al., 1991). Biochemical genetic studies (Petrotta-Simpson et al., 1975; Schwencke and De Robichon-Szulmajster, 1976) suggest that Erc1 might be the yeast *S*-adenosylmethionine vacuolar transporter. It is tempting, therefore, to speculate that the ethionine resistance reported by Shiomi et al. (1991) is conferred by an overaccumulation of *S*-adenosylmethionine toward *S*-adenosylethionine in the vacuole. The DinF protein from *E. coli* belongs to the SOS regulon, a set of genes involved in a variety of activities (SOS response) that protect cells exposed to agents damaging DNA or interfering with its replication. The SOS response includes DNA repair, recombination, and mutagenesis in bacteria (Kenyon and Walker, 1980).

The *TT12* Gene May be Involved in Vacuolar Transport of Flavonoids in the Endothelium Layer of Arabidopsis Seeds

The colors exhibited by flowers and seeds mostly originate from the accumulation of flavonoids in vacuoles. The overall pattern of pigmentation is determined not only by the action of structural and regulatory genes of the flavonoid biosynthetic pathway but also by vacuolar pH, copigmentation, and the shape of the pigmented cell (Mol et al., 1998). The fact that the *tt12* mutant exhibits a strong reduction in PA deposition in the vacuoles of the seed endothelium, together with the homology of the TT12 protein to drug secondary transporters, suggest several hypotheses to explain the mutant phenotype. The first and more probable hypothesis is that TT12 may be a vacuolar transporter for PA precursors (leucocyanidins and catechins), as it is very unlikely that the polymeric procyanidin itself may be handled by a transporter. Therefore, the *tt12* seeds may be dull pale brown because of an accumulation of PA precursors in the cytoplasm. In maize, C-3-G exhibits a bronze color when stored in the cytoplasm of the *bz2* mutant but is purple in vacuoles of wild-type plants (Marrs et al., 1995). The slight vanillin staining observed in *tt12* seeds may result from PA precursors that are handled by transporters other than *tt12* or from residual precursors not yet degraded by the cell machinery. Flavonoids such as flavonols (quercetin and kaempferol) and flavones can act as copigments with anthocyanins, and in so doing, they confer to anthocyanins an increased stability in the acidic vacuolar environment (Mol et al., 1998). This observation leads to the second hypothesis, which is that TT12 would transport copigments for PAs. In the absence of copigments, PA precursors entering the vacuole would not be able to form stable PA polymers and would degrade. Copigments stored in the cytoplasm would degrade as well and contribute, with the vacuolar PA precursors, to the pale brown color of *tt12* seeds. Barz (1977) reported that a peroxidase acting on quercetin could lead to brown degradation products. However, to date, the formation of complexes between PAs and potential copigments has never been reported (Porter, 1993). A third hypothesis would be that TT12 drives the vacuolar sequestration of compounds that interfere with vacuolar pH homeostasis. A possibility is the transport of protons, which is generally

attributed to vacuolar ATPases and pyrophosphatases. However, TT12 does not have any sequence homology with these proteins. Moreover, PAs are stable in neutral or basic conditions, and the activity of the polyphenoloxidase and peroxidase enzymes is reported to be more dependent on the presence of oxygen than on a precise pH (Marbach and Mayer, 1975; Barz, 1977; Egley et al., 1983; Porter, 1992).

Arabidopsis testa pigments are essentially dihydroquercetin (DHQ) derivatives (Chapple et al., 1994), presumably because of a higher enzymatic affinity for these products than for dihydrokaempferol (DHK) derivatives. Indeed, when the supply of DHQ is blocked (as in the *tt7* mutant), the biosynthesis of DHK derivatives is observed (Koornneef et al., 1982; Schoenbohm et al., 2000), although in very small amounts, accounting for the pale brown color of *tt7*. Consequently, *tt7 tt12* seeds would appear unpigmented because of the reduced accumulation of DHK derivatives in the cytoplasm.

The *TT12* gene is expressed specifically in the endothelium layer of ovules and immature seeds. Maximum transcription coincides with the active biosynthesis of PAs and their appearance in vacuoles. The transcript is not detectable after vacuoles are full of PAs. The pattern of *TT12* expression is identical to that of the *BAN* gene described by Devic et al. (1999). *BAN* is postulated to encode a leucoanthocyanidin reductase enzyme (Devic et al., 1999) that catalyzes the formation of catechin from leucocyanidin, both products being procyanidin precursors. The *ban* mutation is mostly epistatic to *tt12*. Together, these data strongly suggest that TT12 may be a transporter for one or both PA precursors, catechin and leucocyanidin. The slight color difference between *ban* and *ban tt12* possibly reveals a capacity of TT12 to transport anthocyanins as well, but to a small extent. These data may provide experimental support for the model proposed by Damiani et al. (1999) in which catechin and procyanidin precursors accumulate in vacuoles before being polymerized to procyanidins.

Flavonoids are synthesized in the cytoplasm at the level of the endoplasmic reticulum (Burbulis and Winkel-Shirley, 1999) and around the vacuoles (D. Saslowsky and B. Winkel-Shirley, personal communication) before their deposition in other cell compartments. The fact that PAs have been reported to reach the vacuole in vesicles derived from the endoplasmic reticulum (Baur and Walkinshaw, 1974; Parham and Kaustinen, 1977; Zobel, 1986; Ibrahim, 1992) is puzzling. It is possible that these vesicles bring PA precursors to the surface of the tonoplast, where they are handled by a transporter. Therefore, the TT12 transporter may be present in both tonoplast and vesicular membranes. The sorting of secondary metabolites via vesicle-specific transporters has been hypothesized by Grotewold et al. (1998).

In maize aleurone cells, the vacuolar transport of C-3-G may require the addition of a GSH tag by a GST enzyme. This GSH tag would be recognized by the GS-X pump that performs the transport of C-3-G (Marrs et al., 1995; Alfenito et al., 1998). By analogy with this situation, we can imagine that the TT12 transporter also may require a system of molecular tagging. A GSH tag is unlikely, because this system has been found to function only with ABC transporters such as the GS-X pump (Rea, 1999). Glycosyl, acyl, or malonyl decorations are other alternatives and have been observed for catechins (Porter, 1993). The potential role of such decorations as tags is also suggested by diverse studies dealing with the vacuolar uptake of phenolic metabolites by secondary transporters. Klein et al. (1996) reported the vacuolar transport of isovitexin, a flavone glucoside of barley, via an isovitexin/H^+ antiport. Hopp and Seitz (1987) postulated that cyanidin glycosides acylated with sinapic acid were transported into carrot vacuoles by a high-affinity carrier, with a pH gradient across the tonoplast being involved in the uptake mechanism. The slight homology of TT12 with *O*-antigen and succinoglycan transporters may indicate that it has a preference for complex glycosylated substrates. For instance, bacterial *O*-antigen chains, which generally are rich in rhamnose residues (Marie et al., 1998), may resemble the complex glycosylation patterns exhibited by some flavonoids.

Bacteria, which have always been in contact with toxic compounds in their natural environment, have developed a multidrug resistance strategy that is dependent mainly on drug/proton antiporters (Paulsen et al., 1996; Bolhuis et al., 1997). Therefore, we hypothesize that TT12 is of bacterial origin and has adapted to plant cell constraints by detoxifying drugs not through an efflux system, as in bacteria, but through their sequestration in vacuoles. The similarity of TT12 with the transporters Erc1, NorM, and DinF, which act in cell defense against toxic compounds, is informative. At least 30 transporter-like genes of unknown function that are similar to TT12 are present in Arabidopsis. It is tempting to speculate that they may be involved in aspects of cell detoxification as well. Studies with ABC transporters revealed that flavonoid substrate recognition involved not only the glutathione or glycosyl moieties but also the basic C15 core (Klein et al., 2000). Therefore, we can imagine the existence of multiple transporters able to respond to the diversity of flavonoids encountered in a plant cell.

METHODS

Arabidopsis Lines, Germination Assays, and Growth Conditions

Mutant screening was performed on 4900 independent T-DNA transformant lines of *Arabidopsis thaliana* in the Wassilewskija-1 (Ws-1) background obtained as described by Feldmann (1991). The seed lots were obtained from the Arabidopsis Biological Resource Center (Columbus, OH). The alleles of the *transparent testa* (*tt*) mutants *tt1* to *tt14*, the *transparent testa glabra* mutant *ttg1*, and the *banyuls* (*ban*) mutant have been described (Debeaujon et al., 2000). The *tt15-1* mutant was obtained by ethyl methanesulfonate mutagenesis of the Columbia-2 genotype (Focks et al., 1999).

To screen for mutants, we sowed T5 seeds from T4 T-DNA transformant families (49 pools of 100 plants each) and wild-type seeds obtained from plants cultivated in a growth chamber under controlled

environmental conditions (20°C, with continuous lighting provided by 38-W Philips [Eindhoven, The Netherlands] TL 84 fluorescent tubes supplemented with four 60-W incandescent lamps on an area of 2 m^2) 3 weeks after harvest; storage was at room temperature. For each pool, plating of 300 to 500 T5 seed was performed in 9-cm Petri dishes on demineralized water–soaked filter paper (number 595; Schleicher and Schuell, Dassel, Germany) without previous seed sterilization.

The primary dormancy level of the *tt12* mutant compared with wild-type and F1 seeds from reciprocal crosses was assessed with seed lots obtained from plants cultivated in a growth chamber. Seven days after harvest, eight replicates of 80 to 100 seed per genotype were sown on demineralized water–soaked filter paper in 6-cm Petri dishes. Germination was scored after a 7-day incubation in a climate-controlled room (25°C, 16 hr of light per day provided by Philips TL 57 lamps), and the average germination percentages ±SE of eight replicates were calculated.

The climate-controlled room also was used for in vitro cultures. The selection of transformants was done by sowing surface-sterilized T1 seeds on basal Gamborg B5 medium with 1% (w/v) sucrose and 0.8% agar supplemented with 50 mg L^{-1} of either kanamycin (Duchefa, Haarlem, The Netherlands) or hygromycin B (Duchefa). For routine seed production and genetic mapping, plants were grown in the greenhouse and handled under conditions described by Debeaujon et al. (2000).

Genetic Analysis

For mapping, a cross was made between the *tt12* mutant and the marker line W1 harboring one homozygous recessive mutation per chromosome (*an*, *py*, *gl1*, *cer2*, and *ms1*). Two hundred sixty F2 plants originating from this cross were scored for the marker phenotypes as well as the color of their seeds. Because some linkage was observed between *tt12* and the *gl1* marker (only five *tt12 gl1* plants were recovered), a cross was made between *tt12* and the marker line W132 harboring three homozygous recessive mutations distributed equally along chromosome 3 (*hy2*, *gl1*, and *cer7*). A total of 375 F2 plants that originated from this cross were scored; 93 F2 lines with *tt12* seed were screened for the segregation of *cer7*, and only one segregating line was found.

The F2 progeny of crosses of *tt12* with the *tt* mutants *tt1* to *tt15* and *ttg1*, first examined for the presence or absence of seed color complementation, were further exploited for the construction of double mutants. For all mutations except *tt5* and *tt6*, the color of F4 seeds was observed on 24 F3 plants producing either pale brown *tt12* seeds or seeds with the other mutations' characteristics. In the case of *tt5* and *tt6*, which are linked to *tt12*, the color of F4 seeds from 123 and 97 F3 lines, respectively, with pale brown *tt12* seeds was recorded, and eight and 10 plants segregating for *tt5* and *tt6*, respectively, were observed. Recombination percentages were estimated in the F2 generation with the RECF2 program (Koornneef and Stam, 1992) and in F3 by applying the formula proposed by Koornneef and Stam (1992). Map locations were determined with the computer program JoinMap (Stam, 1993) by combining our linkage data with the genetic map described by Koornneef (1994).

Microscopy

Toluidine blue O staining of mature seed cuttings and the vanillin HCl assay were performed as reported by Debeaujon et al. (2000). Observations and photographs were made with an Optiphot light microscope (Nikon, Tokyo, Japan).

DNA Gel Blot Analysis, Plasmid Rescue, and DNA Sequencing

Genomic DNA was isolated from rosette leaves of 3-week-old plants grown in the greenhouse, as described by Kubo et al. (1999). For genomic DNA gel blot analyses, 5 μg of DNA was digested with appropriate restriction enzymes (Gibco BRL Life Technologies, Gaithersburg, MD) according to the manufacturer's instructions. Restriction fragments were separated on an 0.8% agarose gel and blotted to a Hybond N^+ membrane (Amersham Pharmacia Biotechnology, Piscataway, NJ), as recommended by the manufacturer. Probes were labeled with α-^{32}P-dATP using the Random Primers DNA Labeling System (Gibco BRL). Blots were hybridized overnight at 65°C in 5 × SSC (1 × SSC is 0.15 M NaCl and 0.015 M sodium citrate), 5 × Denhardt's solution (1 × Denhardt's solution is 0.02% [w/v] bovine serum albumin, 0.02% [w/v] ficoll, and 0.02% [w/v] polyvinylpyrrolidone), and 0.5% (w/v) SDS, with a final wash at 65°C in a 3 × SSC and 0.1% (w/v) SDS solution for 10 min before autoradiography.

Plant DNA flanking the right border of the T-DNA was isolated by plasmid rescue according to the recommendations of Feldmann (1992). After purification on cesium chloride, 3 μg of genomic DNA from the *tt12* mutant was digested to completion with EcoRI. After phenol-chloroform purification and ethanol precipitation, restriction fragments were allowed to ligate at a dilute concentration (ligation volume of 300 μL) to promote self-ligation using 12 Weiss units of T4 DNA ligase (New England BioLabs, Beverly, MA). After phenol-chloroform purification and ethanol precipitation, the ligation mixture was resuspended in 40 μL of double-distilled water, transformed into *Escherichia coli* strain MC1061 (Stratagene, La Jolla, CA) by electroporation, and plated on Luria-Bertani medium supplemented with 100 μg mL^{-1} ampicillin (Duchefa). Seventy-nine kanamycin-sensitive colonies were recovered and further proved positive after filter hybridization with a T-DNA right border probe. Restriction analysis of the plasmids contained in eight randomly chosen colonies revealed a unique plasmid of 11.6 kb (pEB8). Double digestion of pEB8 with EcoRI and BamHI gave a band pattern that matched the model of a T-DNA inverted tandem repeat whose inverted T-DNA would be truncated around the middle of the pBR322 area. A 3.5-kb SalI-EcoRI band that cross-hybridized with pBR322 and a genomic DNA gel blot of Arabidopsis was subcloned into the pSport1 plasmid (Gibco BRL) to form the pEB8 junction plasmid and sequenced to localize precisely the site of T-DNA insertion.

DNA sequencing was performed on an ABI 373 sequencer (Applied Biosystems, Foster City, CA) after Taq cycle sequencing reaction with universal (Sp6 and T7) and specific primers.

Screening of Genomic and cDNA Libraries

A 1.8-kb EcoRI-BamHI subclone of the pEB8 junction plasmid containing only plant flanking DNA was used to probe a genomic library of the Landsberg *erecta* genotype. The library was constructed by cloning genomic DNA partially digested with Sau3AI in the λ FIX II vector using the λ FIX II/XhoI Partial Fill-In Vector Kit (Stratagene). Before amplification for screening, it was estimated to contain approximately four genomes spread over 26,000 clones of ~15 kb in length (C. Alonso-Blanco and A.J.M. Peeters, unpublished data).

One positive clone was recovered (15.2 kb) and submitted to fine restriction mapping. The first half of the λ clone (to the KpnI site from the left) was used to probe the Gif seed library in the λZAPII vector (Stratagene), which was constructed from developing siliques of ecotype Columbia at all developmental stages (Giraudat et al., 1992). The screening of $\sim 31 \times 10^5$ plaque-forming units per fraction led to the recovery of only one positive clone spanning the site of T-DNA insertion. Restriction fragments of a 4.5-kb genomic area of the λ clone involving the *TT12* cDNA clone position (EcoRI-KpnI subclone) and of the 1.6-kb *TT12* cDNA were subcloned in pSport1 for complete double-strand sequencing.

Complementation of the *tt12* Mutant Seed Color

The 4.5-kb EcoRI-KpnI fragment of the λ genomic clone was inserted at the EcoRI and KpnI sites of the pBIB-HYG binary vector containing a gene that confers resistance to hygromycin in plants (Becker, 1990) to create the pEK45 vector. The pEK45 vector was introduced by electroporation into the C58C1 *Agrobacterium tumefaciens* strain GV3101 containing the plasmid pMP90. Its structure in Agrobacterium was determined by DNA gel blot analysis after BamHI-EcoRI digestion of total Agrobacterium DNA and probing with the complete pEK45 plasmid. The transformed Agrobacterium strain was further used to transform eight *tt12* mutant plants according to the in planta transformation procedure of Bechtold et al. (1993). T1 primary transformants selected on the basis of their resistance to hygromycin B were transferred to the greenhouse to set T2 seeds that were observed for color complementation.

RNA Extraction and Reverse Transcription–Polymerase Chain Reaction

RNA was isolated from various tissues harvested from plants grown in the greenhouse. Exceptions were roots, which came from 10-day-old seedlings grown in vitro on Gamborg B5 medium, 1% agarose, and 10 g L^{-1} sucrose in 9-cm Petri dishes placed vertically and 4-day-old seedlings grown on the same medium. The developmental categories of immature siliques were numbered from 1 to 10 from the top to the bottom of the flowering stem, with each stage involving four subsequent siliques. The prevalent embryo developmental stage of each category was determined by observation of seeds with an Optiphot microscope equipped with Nomarski differential interference contrast optics after clearing in a chloralhydrate:glycerol:water (8:2:1 [v/v/v]) solution. Tissue samples were harvested on several main stems from the same lot of wild-type Ws-1 plants. Total RNA was isolated from tissues ground in liquid nitrogen according to the RNeasy Plant Mini Kit procedure (Qiagen, Hilden, Germany) completed with a DNase I treatment according to the RNase-Free DNase Set protocol (Qiagen).

For quantitative reverse transcription–polymerase chain reaction (RT-PCR), first-strand cDNA was synthesized from 1 μg of total RNA in a volume of 20 μL containing 20 mM Tris-HCl, pH 8.4, 50 mM KCl, 2.5 mM $MgCl_2$, 10 mM DTT, 1 mM deoxynucleotide triphosphate mixture, 500 ng of oligo$(dT)_{12-18}$ (Gibco BRL), 25 units of RNase Out (Gibco BRL), and 200 units of Moloney murine leukemia virus reverse transcriptase SuperScript II (Gibco BRL) for 50 min at 42°C. Two microliters of the first-strand solution previously diluted 10 times was used for PCR reaction in a total volume of 50 μL with 20 mM Tris-HCl, pH 8.4, 50 mM KCl, 1.5 mM $MgCl_2$, 0.2 mM deoxynucleotide triphosphate mixture, 0.2 μM of each gene-specific amplification primer, and 1 unit of Taq DNA polymerase (Gibco BRL). The gene-specific primers tt12-fw (5′-CAGAGGAACTAATAAACGGACC-3′) and tt12-rev (5′-CAGAGTCACTGTTGCTGTTATC-3′) amplified bands of 1.6 kb in the *TT12* cDNA and 2.2 kb in genomic DNA. The polyubiquitin gene *UBQ10* (Callis et al., 1995; GenBank accession number L05361), which is known to be the most constantly expressed in many organs among all of the polyubiquitin genes of Arabidopsis (Sun and Callis, 1997), was used as a positive control for RT-PCR. The gene-specific primers ubq10-fw (5′-AACTTTCTCTCAATTCTCTCT-ACC-3′) and ubq10-rev (5′-CTTCTTAAGCATAACAGAGACGAG-3′) amplified bands of 1.4 kb in the *UBQ10* cDNA and 1.7 kb in genomic DNA. To ensure the linearity of amplification for both genes,we performed PCR with 18, 21, and 24 cycles, each cycle involving 30 sec at 94°C, 30 sec at 60°C, and 2 min, 30 sec at 72°C. The three series fulfilled the linearity requirement, but only the results of the 21-cycle series are shown. The amplified DNA samples were separated on a 1% (w/v) agarose gel and, after alkaline blotting to a nylon Hybond N^+ membrane (Amersham Pharmacia Biotechnology), hybridized to either *TT12* or *UBQ10* cDNA PCR probes. Probe labeling and hybridization conditions were as described for DNA analysis. A final wash at 65°C in a 0.1 × SSC and 0.1% (w/v) SDS solution for 15 min was performed before autoradiography.

In Situ mRNA Hybridization

Nonradioactive in situ detection of RNA expression using digoxigenin-labeled RNA probes was performed as described by Vroemen et al. (1996). The *TT12* antisense and sense RNA probes were transcribed from the pBluescript-SK+ plasmid (Stratagene) containing the *TT12* cDNA using the T7 (antisense) or the T3 (sense) promoter.

Bioinformatics

Sequence analysis was performed with the LASERGENE software package (DNASTAR, Madison, WI). The hydropathy plot was drawn using the DNA Strider 1.3 program according to the method of Kyte and Doolittle (1982). Transmembrane regions were also predicted by the transmembrane hidden Markov model (TMHMM) program (http://genome. cbs.dtu.dk/services/TMHMM/). Database searches for homologous sequences were performed on the BLAST server (http://www.ncbi.nlm.nih.gov/blast). Multiple sequence alignment was performed with CLUSTALW accessible on the BCM Search Launcher (Human Genome Center, Baylor College of Medicine, Houston, TX; http://dot.imgen.bcm.tmc.edu:9331/multi-align/multi-align.html). Shading of multiple alignments was realized with BOXSHADE 3.21 (http://www.ch.embnet.org/software/BOX_form.html). Information on transporter classification was obtained on the Internet site of Milton Saier (http://www-biology.ucsd.edu/~msaier/transport/titlepage2.html).

ACKNOWLEDGMENTS

Maarten de Waard, Elisabeth Vierling, and Vered Raz are gratefully acknowledged for critically reading the manuscript. We thank Valérie Hecht and Ed Schmidt for their help with in situ hybridization experiments, Carlos Alonso-Blanco for valuable discussions during the course of this work, and Gerton van de Bunt for help with mutant

screening. We are also grateful to Jérôme Giraudat for providing us with the Arabidopsis silique cDNA library, to Tony van Kampen for assistance in DNA sequencing, to Andy Pereira for advice on plasmid rescue, to Nicole Focks and Christoph Benning for the gift of *tt15-1* seeds, and to the Arabidopsis Biological Resource Center for providing the Feldmann's T-DNA transformant collection, the λPRL2 cDNA library, and the T-DNA right border probe. This work was supported by the European Community Human Capital and Mobility Program (Grant No. ERB4001GT930753 to I.D.) and the European Community BIOTECH Program (Grant Nos. BIOT-CT90-0207 and BIOT-CT92-0529 to M.K.).

Received September 19, 2000; accepted February 9, 2001.

REFERENCES

Albert, S., Delseny, M., and Devic, M. (1997). BANYULS, a novel negative regulator of flavonoid biosynthesis in the Arabidopsis seed coat. Plant J. **11,** 289–299.

Alfenito, M.R., Souer, E., Goodman, C.D., Buell, R., Mol, J., Koes, R., and Walbot, V. (1998). Functional complementation of anthocyanin sequestration in the vacuole by widely divergent glutathione *S*-transferases. Plant Cell **10,** 1135–1149.

Barz, W. (1977). Degradation of polyphenols in plants and plant cell suspension cultures. Physiol. Veg. **15,** 261–277.

Baur, P.S., and Walkinshaw, C.H. (1974). Fine structure of tannin accumulation in callus cultures of *Pinus elliotti* (slash pine). Can. J. Bot. **52,** 615–619.

Bechtold, N., Ellis, J., and Pelletier, G. (1993). *In planta Agrobacterium*-mediated gene transfer by infiltration of adult *Arabidopsis thaliana* plants. C. R. Acad. Sci. Paris **316,** 1194–1199.

Becker, D. (1990). Binary vectors which allow the exchange of plant selectable markers and reporter genes. Nucleic Acids Res. **18,** 203–204.

Bell, A.A., El-Zik, K.M., and Thaxton, P.M. (1992). Chemistry, biological significance and genetic control of proanthocyanidins in cotton (*Gossypium* spp.). In Plant Polyphenols, R.M. Hemingway and P.E. Lacks, eds (New York: Plenum Press), pp. 571–595.

Bolhuis, H., van Veen, H.W., Poolman, B., Driessen, A.J.M., and Konings, W.N. (1997). Mechanisms of multidrug transporters. FEMS Microbiol. Rev. **21,** 55–84.

Brown, M.H., Paulsen, I.T., and Skurray, R.A. (1999). The multidrug efflux protein NorM is a prototype of a new family of transporters. Mol. Microbiol. **31,** 393–395.

Burbulis, I.E., and Winkel-Shirley, B. (1999). Interactions among enzymes of the Arabidopsis flavonoid biosynthetic pathway. Proc. Natl. Acad. Sci. USA **96,** 12929–12934.

Callis, J., Carpenter, T., Sun, C.-W., and Vierstra, R.D. (1995). Structure and evolution of genes encoding polyubiquitin and ubiquitin-like proteins in *Arabidopsis thaliana* ecotype Columbia. Genetics **139,** 921–939.

Camilleri, C., Lafleuriel, J., Macadré, C., Varoquaux, F., Parmentier, Y., Picard, G., Caboche, M., and Bouchez, D. (1998). A YAC contig map of *Arabidopsis thaliana* chromosome 3. Plant J. **14,** 633–642.

Chapple, C.C.S., Shirley, B.W., Zook, M., Hammerschmidt, R., and Somerville, S.C. (1994). Secondary metabolism in Arabidopsis. In Arabidopsis, E.M. Meyerowitz and C.R. Somerville, eds (Cold Spring Harbor, NY: Cold Spring Harbor Laboratory Press), pp. 989–1030.

Coleman, J.O.D., Blake-Kalff, M.M.A., and Davies, T.G.E. (1997). Detoxification of xenobiotics by plants: Chemical modification and vacuolar compartmentation. Trends Plant Sci. **2,** 144–151.

Damiani, F., Paolocci, F., Cluster, P.D., Arcioni, S., Tanner, G.J., Joseph, R.G., Li, Y.G., de Majnik, J., and Larkin, P.J. (1999). The maize transcription factor *Sn* alters proanthocyanidin synthesis in transgenic *Lotus corniculatus* plants. Aust. J. Plant Physiol. **26,** 159–169.

Debeaujon, I., and Koornneef, M. (2000). Gibberellin requirement for Arabidopsis seed germination is determined both by testa characteristics and embryonic abscisic acid. Plant Physiol. **122,** 415–424.

Debeaujon, I., Léon-Kloosterziel, K.M., and Koornneef, M. (2000). Influence of the testa on seed dormancy, germination and longevity in Arabidopsis. Plant Physiol. **122,** 403–413.

Deshpande, S.S., Cheryan, M., and Salunkhe, D.K. (1986). Tannin analysis of food products. CRC Crit. Rev. Food Sci. Nutr. **24,** 401–449.

Devic, M., Guilleminot, J., Debeaujon, I., Bechtold, N., Bensaude, E., Koornneef, M., Pelletier, G., and Delseny, M. (1999). The *BANYULS* gene encodes a DFR-like protein and is a marker of early seed coat development. Plant J. **19,** 387–398.

Egley, G.H., Paul, R.N., Jr., Vaughn, K.C., and Duke, S.O. (1983). Role of peroxidase in the development of water-impermeable seed coats in *Sida spinosa* L. Planta **157,** 224–232.

Feinbaum, R.L., and Ausubel, F.M. (1988). Transcriptional regulation of the *Arabidopsis thaliana* chalcone synthase gene. Mol. Cell. Biol. **8,** 1985–1992.

Feldmann, K.A. (1991). T-DNA insertion mutagenesis in Arabidopsis: Mutational spectrum. Plant J. **1,** 71–82.

Feldmann, K.A. (1992). T-DNA insertion mutagenesis in Arabidopsis: Seed infection/transformation. In Methods in Arabidopsis Research, C. Koncz, N.-H. Chua, and J. Schell, eds (Singapore: World Scientific Publishing), pp. 274–289.

Focks, N., Sagasser, M., Weisshaar, B., and Benning, C. (1999). Characterization of *tt15*, a novel *transparent testa* mutant of *Arabidopsis thaliana* (L.) Heynh. Planta **208,** 352–357.

Giraudat, J., Hauge, B.M., Valon, C., Smalle, J., Parcy, F., and Goodman, H.M. (1992). Isolation of the Arabidopsis *ABI3* gene by positional cloning. Plant Cell **4,** 1251–1261.

Grotewold, E., Chamberlin, M., Snook, M., Siame, B., Butler, L., Swenson, J., Maddock, S., St. Clair, G., and Bowen, B. (1998). Engineering secondary metabolism in maize cells by ectopic expression of transcription factors. Plant Cell **10,** 721–740.

Halloin, J.M. (1982). Localization and changes in catechin and tannins during development and ripening of cottonseed. New Phytol. **90,** 651–657.

Henderson, P.J.F. (1993). The 12-transmembrane helix transporters. Curr. Opin. Cell Biol. **5,** 708–751.

Hopp, W., and Seitz, H.U. (1987). The uptake of acylated anthocyanin into isolated vacuoles from a cell suspension culture of *Daucus carota*. Planta **170,** 74–85.

Hrazdina, G. (1992). Compartmentation in aromatic metabolism. In Phenolic Metabolism in Plants, H.A. Stafford and R.K. Ibrahim, eds (New York: Plenum Press), pp. 1–23.

Ibrahim, R.K. (1992). Immunolocalization of flavonoid conjugates and their enzymes. In Phenolic Metabolism in Plants, H.A. Stafford and R.K. Ibrahim, eds (New York: Plenum Press), pp. 25–61.

Jende-Strid, B. (1993). Genetic control of flavonoid biosynthesis in barley. Hereditas **119,** 187–204.

Kantar, F., Pilbeam, C.J., and Hebblethwaite, P.D. (1996). Effect of tannin content of faba bean (*Vicia faba*) seed on seed vigour, germination and field emergence. Ann. Appl. Biol. **128,** 85–93.

Kenyon, C.J., and Walker, G.C. (1980). DNA-damaging agents stimulate gene expression at specific loci in *Escherichia coli*. Proc. Natl. Acad. Sci. USA **77,** 2819–2823.

Klein, M., Weissenböck, G., Dufaud, A., Gaillard, C., Kreuz, K., and Martinoia, E. (1996). Different energization mechanisms drive the vacuolar uptake of a flavonoid glucoside and a herbicide glucoside. J. Biol. Chem. **271,** 29666–29671.

Klein, M., Martinoia, E., Hoffmann-Thoma, G., and Weissenböck, G. (2000). A membrane-potential dependent ABC-like transporter mediates the vacuolar uptake of rye flavone glucuronides: Regulation of glucuronide uptake by glutathione and its conjugates. Plant J. **21,** 289–304.

Koornneef, M. (1994). Arabidopsis genetics. In Arabidopsis, E.M. Meyerowitz and C.R. Somerville, eds (Cold Spring Harbor, NY: Cold Spring Harbor Laboratory Press), pp. 89–120.

Koornneef, M., and Stam, P. (1992). Genetic analysis. In Methods in Arabidopsis Research, C. Koncz, N.-H. Chua, and J. Schell, eds (Singapore: World Scientific Publishing), pp. 83–99.

Koornneef, M., Luiten, W., de Vlaming, P., and Schram, A.W. (1982). A gene controlling flavonoid 3′ hydroxylation in Arabidopsis. Arabidopsis Inf. Serv. **19,** 113–115.

Kozak, M. (1999). Initiation of translation in prokaryotes and eukaryotes. Gene **234,** 187–208.

Kristiansen, K.N. (1984). Biosynthesis of proanthocyanidins in barley: Genetic control of the conversion of dihydroquercetin to catechin and procyanidins. Carlsberg Res. Commun. **49,** 503–524.

Kubo, H., Peeters, A.J.M., Aarts, M.G.M., Pereira, A., and Koornneef, M. (1999). *ANTHOCYANINLESS2*, a homeobox gene affecting anthocyanin distribution and root development in Arabidopsis. Plant Cell **11,** 1217–1226.

Kyte, J., and Doolittle, R. (1982). A simple method for displaying the hydropathic character of a protein. J. Mol. Biol. **157,** 105–132.

Li, Z.-S., Alfenito, M., Rea, P.A., Walbot, V., and Dixon, R.A. (1997). Vacuolar uptake of the phytoalexin medicarpin by the glutathione conjugate pump. Phytochemistry **45,** 689–693.

Lu, Y.-P., Li, Z.-S., and Rea, P. (1997). *AtMRP1* gene of *Arabidopsis* encodes a glutathione S-conjugate pump: Isolation and functional definition of a plant ATP-binding cassette transporter gene. Proc. Natl. Acad. Sci. USA **94,** 8243–8248.

Lu, Y.-P., Li, Z.-S., Drozdowicz, Y.M., Hörtensteiner, S., Martinoia, E., and Rea, P. (1998). AtMRP2, an Arabidopsis ATP binding cassette transporter able to transport glutathione *S*-conjugate and chlorophyll catabolites: Functional comparisons with AtMRP1. Plant Cell **10,** 267–282.

Mansfield, S.G., and Briarty, L.G. (1994). Endosperm development. In Arabidopsis: An Atlas of Morphology and Development, J. Bowman, ed (New York: Springer-Verlag), p. 385–397.

Marbach, I., and Mayer, A.M. (1975). Changes in catechol oxidase and permeability to water in seed coats of *Pisum elatius* during seed development and maturation. Plant Physiol. **56,** 93–96.

Marie, C., Weintraub, A., and Widmalm, G. (1998). Structural studies of the *O*-antigenic polysaccharide from *Escherichia coli* O139. Eur. J. Biochem. **254,** 378–381.

Marrs, K.A., Alfenito, M.R., Lloyd, A.M., and Walbot, V. (1995). A glutathione *S*-transferase involved in vacuolar transfer encoded by the maize gene *Bronze-2*. Nature **375,** 397–400.

Mol, J., Grotewold, E., and Koes, R. (1998). How genes paint flowers and seeds. Trends Plant Sci. **3,** 212–217.

Morita, Y., Kodama, K., Shiota, S., Mine, T., Kataoka, A., Mizushima, T., and Tsuchiya, T. (1998). NorM, a putative multidrug efflux protein of *Vibrio parahaemolyticus*, and its homolog in *Escherichia coli*. Antimicrob. Agents Chemother. **42,** 1778–1782.

Mueller, L.A., Goodman, C.D., Silady, R.A., and Walbot, V. (2000). AN9, a petunia glutathione S-transferase required for anthocyanin sequestration, is a flavonoid-binding protein. Plant Physiol. **123,** 1561–1570.

Nesi, N., Debeaujon, I., Jond, C., Pelletier, G., Caboche, M., and Lepiniec, L. (2000). The *TT8* gene encodes a basic helix-loop-helix domain protein required for expression of *DFR* and *BAN* genes in Arabidopsis siliques. Plant Cell **12,** 1863–1878.

Parham, R.A., and Kaustinen, H.M. (1977). On the site of tannin synthesis in plant cells. Bot. Gaz. **138,** 465–467.

Paulsen, I.T., Brown, M.H., and Skurray, R.A. (1996). Proton-dependent multidrug efflux systems. Microbiol. Rev. **60,** 575–608.

Pelletier, M.K., and Shirley, B.W. (1996). Analysis of flavanone 3-hydroxylase in *Arabidopsis* seedlings: Coordinate regulation with chalcone synthase and chalcone isomerase. Plant Physiol. **111,** 339–345.

Petrotta-Simpson, T.F., Talmadge, J.E., and Spence, K.D. (1975). Specificity and genetics of *S*-adenosylmethionine transport in *Saccharomyces cerevisiae*. J. Bacteriol. **123,** 516–522.

Porter, L.J. (1992). Structure and chemical properties of the condensed tannins. In Plant Polyphenols, R.W. Hemingway and P.E. Laks, eds (New York: Plenum Press), pp. 245–258.

Porter, L.J. (1993). Flavans and proanthocyanidins. In The Flavonoids: Advances in Research since 1986, J.B. Harborne, ed (London: Chapman and Hall), pp. 23–55.

Rea, P. (1999). MRP subfamily ABC transporters from plants and yeast. J. Exp. Bot. **50,** 895–913.

Rice-Evans, C.A., Miller, N.J., and Paganga, G. (1997). Antioxidant properties of phenolic compounds. Trends Plant Sci. **2,** 152–159.

Saier, M. (2000). A functional-phylogenetic classification system for transmembrane solute transporters. Microbiol. Mol. Biol. Rev. **64,** 354–411.

Sandermann, H., Jr. (1992). Plant metabolism of xenobiotics. Trends Biochem. Sci. **17,** 82–84.

Scalbert, A. (1991). Antimicrobial properties of tannins. Phytochemistry **30,** 3875–3883.

Schoenbohm, C., Martens, S., Eder, C., Forkmann, G., and Weisshaar, B. (2000). Identification of the *Arabidopsis thaliana* flavonoid 3′-hydroxylase gene and functional expression of the encoded P450 enzyme. Biol. Chem. **381,** 749–753.

Schwencke, J., and De Robichon-Szulmajster, H. (1976). The transport of *S*-adenosyl-L-methionine in isolated yeast vacuoles and spheroplasts. Eur. J. Biochem. **65,** 49–60.

Schwetka, A. (1982). Inheritance of seed colour in turnip rape (*Brassica campestris* L.). Theor. Appl. Genet. **62,** 161–169.

Shiomi, N., Fukuda, H., Fukuda, Y., Murata, K., and Kimura, A. (1991). Nucleotide sequence and characterization of a gene conferring resistance to ethionine in yeast *Saccharomyces cerevisiae*. J. Ferment. Bioeng. **4,** 211–215.

Shirley, B.W. (1996). Flavonoid biosynthesis: 'New' functions for an 'old' pathway. Trends Plant Sci. **1,** 377–382.

Shirley, B.W., Hanley, S., and Goodman, H.M. (1992). Effects of ionizing radiation on a plant genome: Analysis of two *Arabidopsis transparent* testa mutations. Plant Cell **4,** 333–347.

Shirley, B.W., Kubasek, W.L., Storz, G., Bruggemann, E., Koornneef, M., Ausubel, F.M., and Goodman, H.M. (1995). Analysis of *Arabidopsis* mutants deficient in flavonoid biosynthesis. Plant J. **8,** 659–671.

Skadhauge, B., Gruber, M.Y., Thomsen, K.K., and von Wettstein, D. (1997). Leucocyanidin reductase activity and accumulation of proanthocyanidins in developing legume tissues. Am. J. Bot. **84,** 494–503.

Stam, P. (1993). Construction of integrated genetic linkage maps by means of a new computer package, JoinMap. Plant J. **3,** 739–744.

Sun, C.-W., and Callis, J. (1997). Independent modulation of *Arabidopsis thaliana* polyubiquitin mRNAs in different organs and in response to environmental changes. Plant J. **11,** 1017–1027.

Todd, J.J., and Vodkin, L.O. (1993). Pigmented soybean (*Glycine max*) seed coats accumulate proanthocyanidins during development. Plant Physiol. **102,** 663–670.

Vroemen, C.W., Langeveld, S., Mayer, U., Ripper, G., Jürgens, G., Van Kammen, A., and De Vries, S.C. (1996). Pattern formation in the Arabidopsis embryo revealed by position-specific lipid transfer protein gene expression. Plant Cell **8,** 783–791.

Walker, A.R., Davidson, P.A., Bolognesi-Winfield, A.C., James, C.M., Srinivasan, N., Blundell, T.L., Esch, J.J., Marks, M.D., and Gray, J.C. (1999). The *TRANSPARENT TESTA GLABRA1* locus, which regulates trichome differentiation and anthocyanin biosynthesis in Arabidopsis, encodes a WD40 repeat protein. Plant Cell **11,** 1337–1349.

Winkel-Shirley, B. (1998). Flavonoids in seeds and grains: Physiological function, agronomic importance and the genetics of biosynthesis. Seed Sci. Res. **8,** 415–422.

Wisman, E., Hartmann, U., Sagasser, M., Baumann, E., Palme, K., Hahlbrock, K., Saedler, H., and Weisshaar, B. (1998). Knock-out mutants from an *En-1* mutagenized *Arabidopsis thaliana* population generate phenylpropanoid biosynthesis phenotypes. Proc. Natl. Acad. Sci. USA **95,** 12432–12437.

Zobel, A. (1986). Localization of phenolic compounds in tannin-secreting cells from *Sambucus racemosa* L. shoots. Ann. Bot. **57,** 801–810.